INVESTIGATING THE EFFECT OF A PROLONGED GAP 1 PHASE ON SPECIFICATION OF PROGENITORS DURING ZEBRAFISH EMBRYOGENESIS

A Thesis
by
Katie Michelle Hahn

Submitted to the Graduate School
Appalachian State University
In partial fulfillment of the requirements for the degree of
MASTER OF SCIENCE

August 2019
Department of Biology

INVESTIGATING THE EFFECT OF A PROLONGED GAP 1 PHASE ON SPECIFICATION OF PROGENITORS DURING ZEBRAFISH EMBRYOGENESIS

A Thesis
by
KATIE MICHELLE HAHN
August 2019

APPROVED BY

_____
Dr. Cortney Bouldin
Chairperson, Thesis Committee

_____
Dr. Andrew Bellemer
Member, Thesis Committee

_____
Dr. Ted Zerucha
Member, Thesis Committee

_____
Dr. Zack Murrell
Chairperson, Department of Biology

_____
Dr. Michael Mckenzie
Dean, Cratis D. Williams School of Graduate Studies

Abstract

INVESTIGATING THE EFFECT OF A PROLONGED GAP 1 PHASE ON SPECIFICATION OF PROGENITORS DURING ZEBRAFISH EMBRYOGENESIS

Katie Michelle Hahn
B.S., Appalachian State University
M.S., Appalachian State University

Chairperson: Dr. Cortney Bouldin

On a grand scale, the process of vertebrate development uses a single-celled zygote to make, through proliferation and differentiation, the many and diverse cells of an adult organism. Decisions to proliferate or differentiate must be tightly regulated, as any errors can cause severe defects. A relationship has been observed between the cell cycle, specifically the gap phases, and a stem cell's decision to remain undifferentiated or differentiate into a specific cell type. While much of what is known about the relationship has been investigated using in vitro and invertebrate models, the zebrafish model provides an excellent system to help better understand the cell cycle and differentiation in vertebrates. Zebrafish, like many other vertebrate species, have a population of posterior progenitor cells, called neuromesodermal progenitors (NMPs), that can become the mesoderm or ectoderm that is needed to form the elongating body. NMPs must make decisions about if and when to divide, as well as when to differentiate in order to provide the cells required for development of the organism.

The *tg(hsp70l:ccnd1DN)* transgenic line, which expresses a mutated form of cyclin D1 under the control of a heat shock promoter, provides a way to manipulate the length of the first gap phase and observe the results on development. Previous and current work in the Bouldin lab has observed the effects of manipulating the cell cycle on NMP differentiation. In order to understand how an altered gap phase affects the critical windows of tissue development during embryogenesis, I determined the timing of heat induced gene expression from the transgene. RNA was present throughout the embryo by 2 hours post heat shock (h pHS) and absent by 4 h pHS. The Ccnd1DN protein was present at 3, 6, and 9 h pHS and was localized to the nucleus. This information will provide the context needed to understand the specifics of how development is affected by a prolonged first gap phase.

NMPs are needed to form ectodermal structures, like the spinal cord and sensory neurons, during embryogenesis. The *Ntrk* family of genes encode receptors that are required for survival of specific populations of sensory neurons in mammals. While most mammals have three, zebrafish have five *ntrk* genes, complicating the question of functionality. I have determined expression of the five *ntrk* genes at two time points in early development, and found that *ntrk1* and *ntrk2a* are expressed by 16.5 hpf and all five *ntrk* genes are expressed by 24 hpf. In order to determine if this expression changed with a prolonged first gap phase, I used the *tg(hsp70l:ccnd1DN)* transgenic line and observed expression of *ntrk2a*. While no significant difference was seen in the number of cells, the size of cells and number of domains of staining was decreased in transgenic embryos, suggesting that there is a relationship between the length of the first gap phase and specification of NMPs.

Acknowledgements

First, I would like to thank my advisor, Dr. Cort Bouldin, for all that he has taught me in the last three and a half years as well as the opportunity he provided me to be the lab's first pancake. I would also like to thank my other committee members, Dr. Andrew Bellemer and Dr. Ted Zerucha, for their guidance, patience, and help with experiments as well as with my writing. I am very thankful for Monique Eckerd for all of her help with the research animals and Dr. Guichuan Hou for his assistance with microscopy. Thank you to current and past members of the Bouldin lab, with special thanks to Jessica Phillips for teaching me how to work in a zebrafish lab, Elsie Rodriguez for her help imaging, and both for their friendship and support. Thank you to King Hung for the data he gathered that provided the foundation of my study. I would also like to extend a special thanks to the Appalachian State University Office of Student Research for the funding they provided for both research and conferences.

Finally I'd like to thank the support system I have been lucky enough to have for the past two years, including all of the graduate students in the Biology Department who are willing to help in any way they can, the professors who are always ready to provide support in the form of advice, ideas, or reagents, and my family for always providing the support I needed to make it through the last two years.

Table of Contents

List of Tables

List of Figures

Foreword

The references, tables and figures within this thesis were prepared in accordance to the author submission requirements of *Development,* a peer-reviewed journal by The Company of Biologists.

INTRODUCTION

The cell cycle and stem cell differentiation

Life depends on the process of cell division. Division of a unicellular organism produces an entirely new organism. In a multicellular organism, cell division allows a single cell to produce the number and diversity of cells found in the adult. From a single-celled human zygote, approximately 37 trillion cells are formed with an estimated 200 different cell types (Bianconi et al., 2013). Going from one cell to trillions requires many decisions to be made, including if and when to divide, as well as when to differentiate. Errors in this process can cause issues for the organism, including cell death and disease, and thus the process must be highly regulated. The highly regulated series of events that allows eukaryotic cells to duplicate their genetic material and divide is known as the cell cycle.

Cell cycle mechanisms are conserved across eukaryotes

In the most basic form of the cell cycle, cells use a synthesis phase, where DNA is replicated and chromosomes are duplicated, followed by mitosis and cytokinesis, where the duplicated chromosomes are packaged into daughter nuclei before the cells split. In addition to synthesis and mitosis, most cells have two gap phases, gap 1 (G1) which follows mitosis, and gap 2 (G2) which follows synthesis. G1 is a very important time for cells, as it is here when cells decide between division or arrest. If cells receive inhibitory signals, G1 acts as a place for cells to pause, also known as arrest. During G2, cells have mechanisms that ensure the DNA was accurately replicated and the proteins necessary for cell division are present.

There are three main checkpoints that exist as stopping points to ensure DNA is replicated accurately and that cells are replicating only as needed: the G1/S checkpoint, the G2/M checkpoint, and the metaphase to anaphase transition (Morgan, 2007). Progression through each checkpoint is highly regulated by two main components: cyclin-dependent kinases (Cdks) and cyclins. Cdks require cyclins to become active which allows progression through the cell cycle to be tightly regulated.

The fundamental components and regulatory elements of the cell cycle are well conserved among eukaryotes (Morgan, 2007). Our understanding of the most basic components of the cell cycle and how cells progress through it comes from studying many different eukaryotic organisms and cell types. Because the eukaryotic cell cycle is well conserved, scientists have the advantage of using different organisms, each with their own specific advantages, to learn about the core components and regulation of the cell cycle. Two organisms that have been critical to what we know about the cell cycle so far are the single-celled yeasts, *Saccharomyces cerevisiae* and *Saccharomyces pombe*. Much of the early work done with yeasts was done before the distinction had been made between prokaryotes and eukaryotes, so they were largely chosen for their ease of use, not their representation of a eukaryotic cell (Mitchison, 1990).

Insights into cell cycle regulation from *Saccharomyces*

Yeasts have been an important tool for studying the cell cycle because of the ease of genetic analysis they provide, as well as the ease of culturing them in a lab. Both organisms have a cell cycle time of approximately 90 to 120 minutes, giving them a clear advantage as

model organisms in terms of time efficiency (Forsburg and Nurse, 1991), as human cells take approximately 24 hours to divide in culture (Cooper, 2000). Yeasts have played an important role in the discovery of many of the specific components of the cell cycle by allowing for the mutation of genes required for division.

The process of studying cell division cycle (*cdc*) genes to investigate their specific roles was more complicated than simply mutating the genes, as cells could not be propagated if the cell cycle was halted due to these mutations (Morgan, 2007). The solution came by use of conditional mutants by Horowitz and Leupold, who showed in T4 bacteriophages that temperature-sensitive mutants could be used to conditionally inactivate genes that were indispensable for viability (Hartwell, 1967; Horowitz and Leupold, 1951). Conditional mutants can be shifted from permissive conditions in which they exhibit a wildtype phenotype to restrictive conditions, at which point the mutant phenotype can be seen (Griffiths et al., 2000). Restrictive conditions will cause an arrest at the point in the cell cycle where the *cdc* gene is required, giving information about functionality. When a temperature-sensitive *S. cerevisiae cdc16* mutant is grown at restrictive temperatures, cells arrest in mitosis which can be determined by the size of the bud. More specifically, a cell arrested in metaphase can be determined by the short metaphase spindle and unsegregated chromosomes (Figure 1). Through genetic analysis, CDC16 has been shown as part of the Anaphase Promoting Complex (APC), which is required for the metaphase to anaphase transition (Zhang et al., 2013), supporting the results observed using conditional mutants.

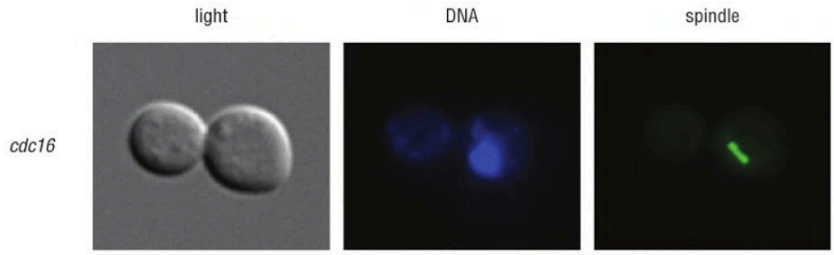

Figure 1. *cdc16 S. cerevisiae* mutants arrest in mitosis before the transition to anaphase. When temperature-sensitive *cdc16 S. cerevisiae* is grown at restriction conditions, cells arrest in metaphase, determined by the short metaphase spindle (from *The Cell Cycle: Principles of Control*, pictures by Greg Tully).

Leland Hartwell was responsible for much of the early screening of *S. cerevisiae* mutants and screened about 400 temperature-sensitive mutants in 1967 (Hartwell, 1967). Between the 1967 screen and another mutant screen in 1970, many *S. cerevisiae cdc* mutants were identified and characterized including a cell cycle factor called *cdc28* (Hartwell et al., 1970). *cdc28* is known to encode Cdk1, the only cyclin-dependent kinase required for survival of both *S. cerevisiae* and *S. pombe* (Budirahardja and Gonczy, 2009). A similar screen was performed with *S. pombe*, although many scientists at the time thought of *S. pombe* as a less important, minor organism. Paul Nurse led this effort in the mid-1970's in the lab of Murdoch Mitchison. One of the *cdc* mutants discovered was *cdc2*, which was determined to encode a Cdk1 homolog, as *cdc28* from *S. cerevisiae* could rescue the defect in a *cdc2* mutant from *S. pombe* (Nurse et al., 1976). Nurse reasoned that as distantly related as these organisms were from each other, it was likely that other organisms (like humans) have homologous genes with a similar function. Melanie Lee and Paul Nurse were able to isolate a *cdc2* homolog from human and show that it was able to rescue the defect in a *S. pombe cdc2*

mutant (Lee and Nurse, 1987). Paul Nurse, Leland Hartwell, and Tim Hunt (for his discovery of the cyclin) were awarded the 2001 Nobel Prize in Physiology or Medicine.

Insights into cell cycle regulation from *Xenopus*

Further studies of the cell cycle control system came from *Xenopus laevis*, or the African clawed frog. Like many animals, *Xenopus* undergoes cleavage early in development. The fertilization of the egg starts the first twelve rounds of cell division, consisting only of mitosis and synthesis, with gap phases absent. The cellular materials required for these first twelve divisions must be stored in the egg, as the onset of zygotic transcription has not yet begun (Philpott and Yew, 2005). Accessibility of the cellular material made *Xenopus* zygotes an excellent organism to study early divisions, as all of the RNA and most of the proteins required for the first twelve divisions were present. Because early divisions are not regulated by many of the checkpoints that cells must go through later in development, the basics of the cell cycle can be studied without checkpoints causing cells to arrest (Lohka et al., 1988).

Early rounds of division are synchronous and undergo periodic global cytoplasmic movements known as surface wave contractions (Hara et al., 1980). Synchrony continues, even when individual blastomeres are separated, raising the question of what kind of mechanism keeps time in cells, and how that information is passed to daughter cells after division. To learn more about the contractions in *Xenopus* embryos, Koki Hara, Peter Tydeman, and Marc Kirscher (1980) used time-lapse imaging to observe contractions and measure the height of the eggs, as periodic rounding and flattening is seen. They compared the results to eggs treated with antimitotic drugs like colchicine and vinblastine, and found

the contractions continued, although cells no longer divided. Even further, cells were tied with human hair to split them into one section containing the nucleus and one section enucleated, and the surface contractions continued at regular intervals in both compartments suggesting the presence of an autonomous cell cycle oscillator, or clock, present in cells. The oscillations that were observed continued even with severe damage or absence of the nucleus. While it was not understood what was causing the oscillations in *Xenopus embryos*, the data pointed to an autonomous regulator that was triggered by fertilization and was independent of the nucleus (Hara et al., 1980).

The discovery of the specific cell cycle factor that causes oscillations in the cell came from studying the maturation of a *Xenopus* embryo. The process of maturation for *Xenopus* oogonia, or immature germ cells of the female reproductive system, involves the replication of DNA and then 8 months of G2 arrest while the oogonium grows in size. In order for oogonia to come out of G2 arrest and move into meiosis I, progesterone is secreted by female ovarian cells, and the oogonia undergo a process of maturation, at which time they are referred to as eggs. To study the maturation process in vitro, scientists removed G2 arrested oogonia from the ovary of a frog and treated the oogonia with progesterone to encourage maturation. After exposure to progesterone, oogonia move through meiosis I, interphase, and arrest during metaphase II (Lodish et al., 2000). The cytoplasm from the eggs arrested in metaphase II was then injected into immature oogonia. Even though the immature oogonia had never been exposed to progesterone, they were able to mature into eggs (Figure 2). The cytoplasmic factor required for maturation of oogonia was called maturation promoting factor, or MPF, and was discovered by Yosio Masui and Clement Markert in 1971. MPF is now known as mitosis promoting factor as it has been found as an inducer of mitosis as well

as maturation, and is a complex made up of Cdk1 and cyclin B (Duesbery and Woude, 1998). MPF activity cycles as cells move through the phases of the cell cycle, rising in G2, peaking as cells enter mitosis, and decreasing for the duration of mitosis, causing the clock-like surface contractions that had been previously observed (Murray and Kirschner, 1989).

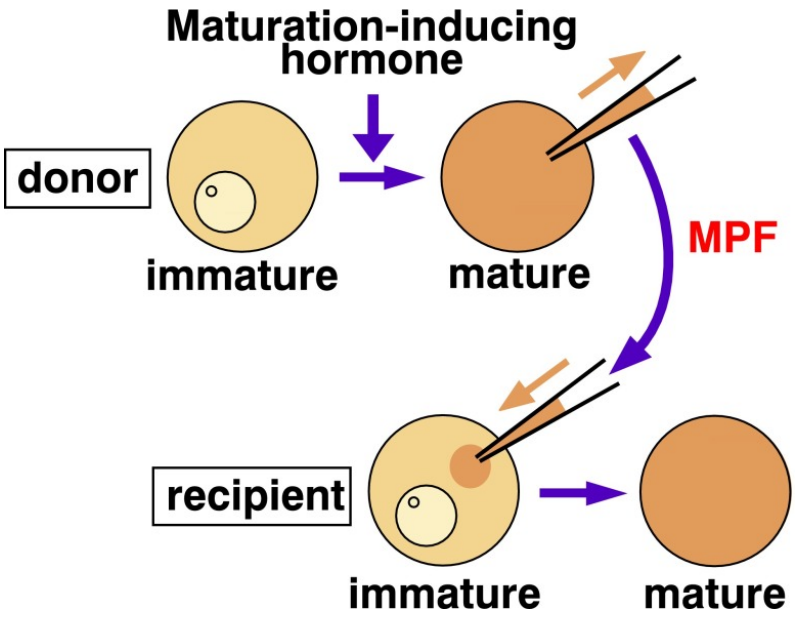

Figure 2. Cytoplasmic injections from mature frog oocytes allowed immature eggs to mature. When cytoplasm was removed from a mature embryo arrested in G2 and injected into an immature recipient, the oocytes matured, even in the absence of progesterone (Kishimoto, 2015).

The unidirectional eukaryotic cell cycle

Eukaryotic cells rely on a highly regulated cell cycle control system to ensure there is coordination in timing and order for cells to proceed through the cell cycle in one direction only, and to ensure that the next events to do not occur until the previous phase is complete. In addition, it is critical that chromosomes are duplicated only once, and that duplicated

chromosomes are evenly distributed between the cells. Because of its importance, the cell cycle control system is intricate and layered, and must be ready to react when something goes awry.

One of the most fundamental aspects of the cell cycle control system is the protein heterodimer complex which consists of a cyclin-dependent kinase (such as Cdk1) and a cyclin (like cyclin B) that controls progression through the cell cycle. Cdks are serine/threonine protein kinases which catalyze the attachment of phosphate groups to protein substrates. Cdks are inactive when not phosphorylated and not bound by a cyclin, their primary regulator (Morgan, 1995). Cyclins are classified based on the phase or transition they are associated with and thus aptly named G1, G1/S, S, or M cyclins. While Cdk levels remain stable throughout the cell cycle, cyclins are only synthesized prior to when they are needed which allows Cdk activity to cycle based on the phase of the cell cycle (Yasutis and Kozminski, 2013). In order to make sure the cell only experiences the cycle in one direction, each cyclin-Cdk complex is involved in the activation of the next phase's cyclin-Cdk complex. Inhibiting expression of cyclins, increasing the rate of cyclin degradation, and increasing the presence of Cdk inhibitors control timing to ensure progression of the cell cycle in one direction (Yasutis and Kozminski, 2013).

The start of a new cell cycle begins in G1 when signals trigger the start point of the cell cycle. Before this point, G1/S, S, and M-Cdks are all inactive to ensure that the cell does not enter a new cell cycle prematurely. The decision to divide can be due to signals inside the cell like the availability of nutrients and growth factors, or outside the cell by the signaling of a mitogen (Morgan, 2007). Commitment to division by the cell triggers expression of G1/S and S cyclins. The main function of G1/S-cyclins is to activate S-Cdks which requires

termination of the mechanisms in place during G1 to keep S-Cdks inactive. Cdk inhibitor proteins (CKIs) are targeted for destruction to allow cells to progress out of G1 into S phase. S-Cdks are then able to phosphorylate target proteins involved in progressing cells into synthesis. G1/S-Cdks can stimulate the destruction of G1/S-cyclins once cells proceed into synthesis (Yasutis and Kozminski, 2013).

By the end of S phase, M-cyclin expression is active leading to an increase in the presence of activated M-Cdks, which are kept inactive by inhibitory phosphorylation until the beginning of mitosis. Active M-Cdks are responsible for activation of the APC, which in addition to its function in destruction of M and S-cyclins, also helps to stimulate the destruction of proteins that hold the sister chromatids together, thereby leading to the metaphase-to-anaphase transition. As M and S-cyclins are targeted for destruction and CKI production is increased, the required dephosphorylation of mitotic targets allows for the completion of mitosis. After mitosis, cyclins are kept at low levels until the end of G1, when the process starts over (Graña and Reddy, 1995).

In addition to cyclin binding, Cdks require phosphorylation in order to become fully active. Cdk phosphorylation happens by a Cdk-activating kinase (CAK) at a conserved threonine residue which is located at a varying position adjacent to the kinase active site. In vertebrates, one CAK has the ability to activate all major Cdks. Cdk phosphorylation works by inducing a conformational change to enhance cyclin binding (Vermeulen et al., 2003).

Inhibitory phosphorylation can prevent the activity of a Cdk/cyclin complex. Cdk1 forms a heterodimer with cyclin B, but is not active until the phosphatase Cdc25 dephosphorylates a specific tyrosine residue (Morgan, 1995). As Cdk1 controls a cell's entry into mitosis, Cdc25 is required for cells to progress through G2 and into mitosis. The activity

of Cdc25 is opposed by the kinase Wee1, and so the ratio of Cdc25 to Wee1 is an important factor in the timing of a cell's entry into mitosis (Gould and Nurse, 1989; Harvey et al., 2005). Cdc25 is highly available in the early embryo, with a decline in levels at the mid-blastula transition (Edgar and Datar, 1996). Once Cdc25 is expressed and can dephosphorylate Cdk1, cells progress through the G2/M transition into mitosis where levels of M-, S-, and G1-cyclins begin to decline until G1.

During early G1, Cdk4/6 is bound by cyclin D (1, 2, and 3). The Cdk4/6-cyclin D complexes then phosphorylates the tumor suppressor retinoblastoma protein (Rb), which allows the transcription factor E2F to be released. Release of E2F leads to transcription of cyclin A and E, both of which are important for G1/S transition and S phase. Cdk2-cyclin E continues to phosphorylate Rb, which continues to release E2F to move cells into S phase, continuing the cycle. The highly regulated nature of the cell cycle begins from the first division, although the regulatory elements and phases of the cell cycle differ early in development (Budirahardja and Gonczy, 2009).

Developmental changes to the cell cycle

Cells early in development use a modified cell cycle, which uses synthesis and mitosis rather than all four phases. During early embryogenesis of many species, cells undergo a cleavage phase which involves rapid mitotic division of cells. During the cleavage phase, cells divide quickly and synchronously to increase cell numbers. Transcription is not required in these early divisions, as they are controlled by maternal genes. The depletion of

maternal factors is concomitant with the beginning of zygotic transcription, which is known as the mid-blastula transition (MBT).

The MBT is where the first gap phase is introduced in most species. In *Drosophila*, *Xenopus,* and zebrafish, a G2 phase is introduced at the MBT. In *Drosophila*, this occurs in cycle 14, when degradation of *string* and *twine*, which are two maternal *cdc25* homologs, cause reduced Cdk1 activity. This can also be seen in zebrafish and *Xenopus*, as a G2 phase is introduced at the MBT regulated by *cdc25* homologs. When *cdc25* mRNA is injected into a zebrafish zygote, results are lethal, demonstrating the importance of the tight regulation of *cdc25* expression in embryonic development (Nogare et al., 2007).

Cells eventually reach a point in development when the cell cycle consists of all four phases. G1 plays an important role in development, as it is often involved in regulating organogenesis. Differentiating cells are often in a quiescent G1 state before terminally differentiating or undergoing another division (Escudero and Freeman, 2007). For example, in *Drosophila* the G1/S transition is important for the development of the eyes as all cells of the eye imaginal disc are held in G1 before either differentiating into photoreceptors or going through one more round of mitosis (Budirahardja and Gonczy, 2009; Escudero and Freeman, 2007).

Because G1 has been seen to play such an important role in development, especially in the process of stem cells differentiating, understanding the relationship between the cell cycle and stem cells can help provide insight into the decision-making process of stem cells during embryogenesis. Stem cells give rise to all the cell types found in an adult organism, and understanding how stem cells make decisions about proliferating to generate more stem

cells, or differentiating to become a specified cell type is imperative for our understanding of the growing body in early development, as well as homeostasis in adulthood.

Embryonic stem cell differentiation: Pluripotency and the cell cycle

The isolation of embryonic stem cells from a mouse blastocyst was an important first step in our ability to study stem cells, including studies of how cells are maintained in a pluripotent state as well as the signals needed for differentiation (Evans and Kaufman, 1981; Martin, 1981). The ability to study stem cells in vitro has greatly increased our understanding of the genes and signaling pathways that play important roles in the maintenance of pluripotency versus differentiation of stem cells. For embryonic stem cells, signaling pathways like Notch, TGF-β, Wingless/Wnt, and Hedgehog are important for regulating pluripotency versus differentiation (Liu et al., 2008). The balance between differentiation and proliferation of stem cells must be tightly regulated as differentiation without proliferation causes a depletion of the stem cell pool while proliferation without differentiation leads to unnecessary division and possibly a tumor.

As cells differentiate, they are fated to one of the three germ layers: mesoderm which forms the blood, heart, muscles, connective tissues, and bones; ectoderm, which generates the epidermis, brain, and nervous system; or endoderm, which produces the epithelium of the digestive tube and its associated organs (Gilbert, 2000). The mechanisms of differentiation in embryonic stem cells (ESCs) vary between organisms. A previous study has shown that mouse embryonic stem cells (mESCs) do not require active signaling of pluripotency factors to maintain pluripotency, and instead only require the lack of differentiation signals or a

balance between signaling pathways that repress differentiation, like LIF (leukemia inhibitory factor)-blocking mesendoderm (a common progenitor of both mesodermal and endodermal cells) and BMP (bone morphogenetic protein)-blocking neuroectoderm (Ying et al., 2008). In contrast, human embryonic stem cells (hESCs) require Activin/Nodal and fibroblast growth factor (FGF) signaling working together to maintain pluripotency factors like Nanog and block neuroectoderm differentiation (Pauklin and Vallier, 2015).

G1 plays an important role in cell fate decisions as a cell's ability to differentiate varies during this phase. BMPs are a family of proteins in the TGF-β superfamily that play an important role in early development, including in embryogenesis, cell differentiation, and cell proliferation (Beederman et al., 2013). In canonical TGF-β signaling, TGF-β forms a complex with proteins in the activin receptor-like kinase family which allows for recruitment and phosphorylation of Smad2/3. Smad complexes can then interact with specific transcription factors, coactivators, and corepressors to regulate gene expression, including cell differentiation (Holtzhausen et al., 2014) in a cell cycle-dependent manner. In early G1, cells are able to initiate endoderm signals when levels of cyclin D are low and Smad2/3 can bind to activate endoderm genes (Pauklin and Vallier, 2013). In late G1, when levels of cyclin D are high, cells are able to initiate neuroectoderm signals, but are no longer able to differentiate into ectoderm. Cyclin D1 is able to form a complex with transcription factors to recruit transcriptional activators onto neuroectoderm genes and repressors onto endoderm genes (Pauklin et al., 2016). When CDK4/6 is inhibited in hESCs in order to prolong G1, more cells differentiate into endoderm due to the increased proportion of cells in early G1 (Pauklin and Vallier, 2013).

Neurogenesis and the cell cycle in the embryonic vertebral spinal cord

Cells of the spinal cord come from a population of neuromesodermal progenitors (NMPs) that play an important role in posterior body elongation. Cells that form the caudal neural plate are under the control of FGF, which is repressed by retinoic acid (RA) produced by the cells that form the neural tube (Olivera-Martinez and Storey, 2007). The cells that will contribute to the spinal cord remain undifferentiated in the epiblast until FGF signaling decreases as the body axis elongates (Akai et al., 2005). The somites, or developing body segments, will then produce RA that inhibits FGF and Wnt signaling which allows the switch from an undifferentiated to a more mature state (Bertrand et al., 2000; Diez del Corral et al., 2002). The neural tube is formed from an involution of the neural plate (Gilbert, 2000). The cells of the caudal neural plate and neural tube express different cell cycle regulators, even though they are both actively proliferating. Cyclin D2 is expressed in the immature caudal neural plate whereas cyclin D1 is expressed in the maturing neural tube, which (Lobjois et al., 2004). While Cdc25a is expressed in both locations, Cdc25b is not expressed in the caudal neural plate (Bénazéraf et al., 2006; Molina and Pituello, 2017).

In the neural tube, Wnts, BMPs, and Sonic Hedgehog (Shh) are linked to the presence of cell cycle machinery and help determine symmetric versus asymmetric divisions of progenitors. Wnt signaling is involved in neural progenitor proliferation, with Wnt1 and Wnt3a positively regulating cell cycle progression by regulating cyclin D1 and cyclin D2 transcription (Megason and McMahon, 2002). BMPs are involved in production of symmetric divisions producing two progenitor cells. A decrease in BMP activity causes a switch to asymmetric divisions producing one progenitor and one neuron, and then symmetric divisions producing two neurons (Dréau et al., 2014). Shh acts upstream of Wnt

signaling to promote proliferation and survival in the neural tube, as well as regulating cyclin D1 expression to promote progression through G1 and regulating the length of G2 by controlling expression of cyclin A, cyclin B, and Cdc25b (Molina and Pituello, 2017).

Adult neurogenesis

While neurogenesis was long thought to happen only in early development, the discovery by Altman and colleagues that neurogenesis continued into adulthood (Altman and Das, 1965) implied the existence of adult neural stem cells. In the adult rodent brain, there are two regions where neurogenesis occurs: the subventricular zone (SVZ) which generates olfactory bulb interneurons, and the subgranular zone which generates granule cells of the dentate gyrus (Figure 3; Farioli-Vecchioli et al., 2014). In these regions, the balance of proliferation versus differentiation is important for ensuring differentiation of enough specialized neuronal cells to maintain function while not depleting the stem cell pool required for this task. The balance is achieved by control of the switch from proliferation to asymmetric and then symmetric division of these cells. Cell cycle regulation is thought to be a key player in this decision-making process (Lange et al., 2009).

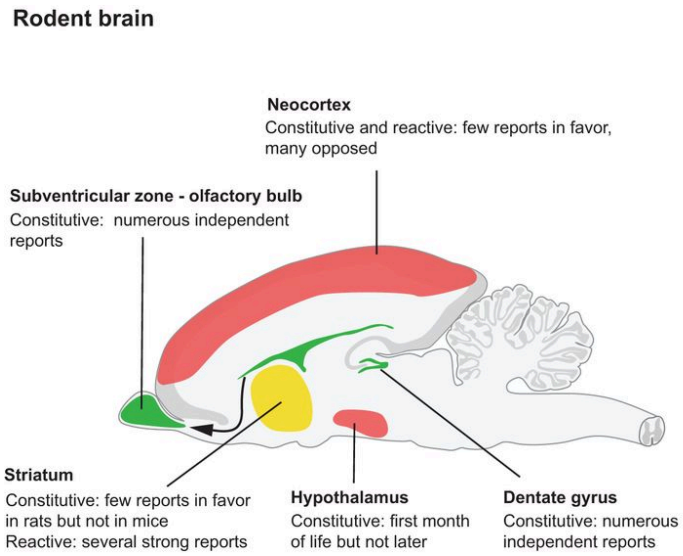

Figure 3. Anatomy of neurogenesis in the adult rat brain. Regions shown in green can go through neurogenesis throughout the life of the organism. Regions in yellow and red have limited or no ability for neurogenesis in adults (Magnusson and Frisén, 2016).

The length of the cell cycle has been shown as an important determinant of neurogenesis, with cortical regions that have a higher proportion of neurogenic divisions found to have cells with a longer G1 (Lukaszewicz et al., 2005). In addition, there have been multiple reports of a relationship between neurogenesis and cell cycle inhibition including overexpression of antiproliferative genes promoting neurogenesis (Canzoniere et al., 2004) and cell cycle inhibitors being used as markers of neurogenetic progenitors (Georgopoulou et al., 2006; Lange et al., 2009). While a correlation can be seen between the cell cycle length and neurogenesis, it remains to be determined whether this increase in the length of G1 is a cause or a consequence of neurogenesis.

In support of the idea that the increase in G1 causes neurogenesis, lengthening G1 by inhibiting the Cdk2/cyclinE1 complex was found to cause premature neurogenesis. This finding led to the formation of the cell cycle length hypothesis which says that the time spent

in G1 must extend past a threshold in order for cells to have sufficient time for fate-determining factors to take effect (Hardwick et al., 2015). So, the increase of the length of G1 would be a cause of neurogenesis, and a short G1 would not allow the time required for the switch to neurogenesis. The cell cycle length hypothesis was further supported by work by Lange et al. (2009), in which the length of G1 in neural progenitors was shortened and the switch from proliferation to differentiation was inhibited, while lengthening the G1 in neural progenitors promoted the switch from proliferation to differentiation. In addition, when the length of G1 was shortened by Cdk4/cyclinD1 overexpression, an increase of basal progenitors (BP) were seen without a proportional change in the apical progenitors (AP), which is consistent with the idea that a shorter G1 causes the neurogenic APs to divide and produce one AP and one BP instead of one AP and one neuron, thereby increasing divisions of progenitor cells instead of differentiated neurons (Lange et al., 2009). Both of these study provide support for the cell cycle length hypothesis as a longer G1 was associated with a switch to differentiation, while a shortened G1 was associated with an increase in proliferative divisions.

It is clear that a relationship exists between the cell cycle and stem cell differentiation. Both of these processes are tightly regulated and vital for development. Understanding this relationship is imperative for understanding embryogenesis. As much of our understanding is based on cell culture or invertebrates like *Drosophila* or *C. elegans*, studying this in vivo in a vertebrate organism provides details that are currently lacking. For example, Pauklin and Vallier showed that the capacity of cells to differentiate varies during different phases of the cell cycle, and these decisions are made within a narrow window of time in G1 (Pauklin and Vallier, 2013). While this study provided an important insight into

mechanisms linking the cell cycle and differentiation, it was performed in vitro using human embryonic stem cells, so the findings may not be consistent with in vivo studies. Using an organism like zebrafish for in vivo studies will allow for a better understanding of the relationship between the cell cycle and stem cell differentiation in vertebrates.

Studying the cell cycle and differentiation in zebrafish

The goal of this project is to investigate the effect of manipulating the cell cycle, specifically prolonging the gap 1 phase, on specification of progenitors during zebrafish embryogenesis. Zebrafish are an excellent model organism for studying many areas of biology, but can be especially advantageous in the study of development and embryogenesis. These tropical fish are small and relatively inexpensive to maintain while still providing a vertebrate model with high genetic similarity to humans (~70% of disease-causing genes in humans have zebrafish homologs; Santoriello and Zon, 2012).

The usefulness of zebrafish extends past their genetic similarity to humans, as they are externally fertilized so embryos can be collected and manipulated at the single cell stage, or eggs and sperm can be collected separately for in vitro fertilization. In addition, large numbers of embryos can be collected, as zebrafish are capable of fertilizing 200-300 eggs every 5-7 days. The embryos are transparent which is beneficial for uses with fluorescent or colored reporters and live imaging experiments. They also provide the benefit of a short time of development, with less than a week being required for the development the cardiovascular, nervous, and digestive systems (Bootorabi et al., 2017). Because of their ease of manipulation, zebrafish have become a common alternative to mice when it comes to generating transgenic organisms. This makes zebrafish a valuable tool for studying the gap phases of the cell cycle and how effects of their manipulation on the cells that form the body during embryogenesis.

Posterior progenitiors in zebrafish

Zebrafish, similarly to other vertebrates, contain a population of bipotential progenitors in the tailbud that continue to specify mesoderm even after gastrulation called neuromesodermal progenitors (Kondoh and Takemoto, 2012). NMPs can remain in the tailbud as bipotential cells or leave the tailbud to make neural and mesodermal fate decisions (Martin and Kimelman, 2012). During the formation of the posterior body of the zebrafish, NMPs form the spinal cord, sensory neurons, vasculature, notochord, and somites. Somite cells are then able to produce tissues such as bone, dermis, and muscle (Aoyama and Asamoto, 1988).

Zebrafish NMPs have a specific cell cycle profile that consists of a relatively short G1 and a prolonged G2 phase required for normal development (Bouldin et al., 2014). During gastrulation NMPs actively divide then become quiescent during somitogenesis until differentiation is required. Ectopic expression of Cdc25, which forces cells out of G2 and into mitosis, was found to inhibit mesodermal differentiation and cause a decrease in the number of somites formed as well as a decrease in total muscle mass (Bouldin et al., 2014).

The development of sensory neurons with *NTRK* genes

While it is clear that NMPs have a specific cell cycle profile required for normal development of muscle, the effects on development of ectodermal structures like the spinal cord and sensory neurons is less well understood. NMPs in the zebrafish tailbud provide an advantageous system for examining the effects of cell cycle manipulation on stem and progenitor cells in vivo. A subset of NMPs are fated to become sensory neurons, including

mechanoreceptors, proprioceptors, and nociceptors, and expression of these neurons provides valuable information on how NMPs contribute to neurogenesis during early development.

Sensory neurons are responsible for sensing an organism's environment as well as protecting it from harmful stimuli. Mechanoreceptors are neurons that sense mechanical stimuli to provide information about touch, pressure, and vibration, proprioceptors provide information about the positioning of the body in space, and nociceptors sense harmful stimuli to initiate the sensation of pain (Purves et al., 2001). In order for neurons to survive, expression of the *Ntrk* genes, or neurotrophic receptor tyrosine kinase genes, is required. Most vertebrates (including mammals) have three *Ntrk* genes, *Ntrk1*, *Ntrk2*, and *Ntrk3* which encode Trk receptors (TrkA, TrkB, and TrkC), which are activated by neurotrophin ligands. Nerve growth factor (NGF) binds to TrkA, brain-derived neurotrophic factor (BDNF) and neurotrophin-4 bind to TrkB, and neurotrophin-3 binds to TrkC. The Trk receptors and ligands are produced by different cells, and both must be present for survival of the neuron (Huang and Reichardt, 2001). Functionality of the Trk receptors was determined using knockout experiments in mice. Knockout of TrkA reduced the number of nociceptors, knockout of TrkB reduced the number of mechanoreceptors, and knockout of TrkC reduced the number of proprioceptors, leading to a modular model of function, where expression of a Trk receptor was responsible for a specific subset of sensory neurons (Reichardt and Fariñas, 1998).

Unlike mammals, zebrafish have five *ntrk* genes (*ntrk1*, *ntrk2a*, *ntrk2b*, *ntrk3a*, and *ntrk3b*), and so five Trk receptors (TrkA, TrkB1, TrkB2, TrkC1, and TrkC2) due to a whole-genome duplication event that happened more than 300 million years ago in the teleost lineage (Glasauer and Neuhauss, 2014). The additional Trk receptors found in zebrafish have

complicated the question of functionality. When a paper, published in 1995, showed the presence of five Trk receptors in zebrafish, the idea was introduced that each receptor was functionally distinct due to differential expression (Martin et al., 1995). More extensive studies determining expression of the *ntrk* paralogs continue to show differential expression, as well as regions of overlap. For example, one study showed that TrkC2 expression was found in two locations of the hindbrain while TrkC1 showed no hindbrain expression but both TrkC1 and TrkC2 were expressed in the telencephalon (Martin et al., 1998). A more recent study found expression of *ntrk3a* in the hindbrain but not *ntrk3b* and suggested that due to the expression in the otic vesicle the *ntrk3* genes were involved in the maintenance of mechanoreceptor progenitors, instead of proprioceptors like in mammals (Nittoli et al., 2018). Another study concluded that all of the Trk receptors in zebrafish were functionally similar, and all involved in the survival of nociceptors, due to their overlapping expression with *trpa1b* and *trpv1*, which are two important nociceptive ion channels, although this study did not take TrkB2 or TrkC2 into consideration (Gau et al., 2017). As the *ntrk* genes play such an important role in the development of the nervous system and can act as specific markers of terminally differentiated sensory neurons, understanding their function is of great interest to many people. The discrepancies and differences in conclusions about these genes show the importance of continuing to study them as well as the difficulty in determining functionality of genes, even just from one vertebrate species to another.

The *Ntrk* genes are vital for normal neurogenesis, as expression is necessary for sensory neuron survival, and thus can act as genetic markers of terminally differentiated neurons. Because of the conflicting data currently available about the *ntrk* genes in zebrafish, I elected to study the expression of the five *ntrk* genes during zebrafish embryogenesis by

looking at two time points in early development to get a better understanding of the functionality of sensory neurons specified by NMPs. Determining expression patterns is an important first step to answer the question of functionality. This also provides a way to determine the order in which these gene are first expressed, by looking at a time point associated with the earliest differentiation of neurons (Kimmel et al., 1995; Metcalfe and Westerfield, 1990).

In addition to looking at the expression of *ntrk* genes in wildtype zebrafish, these genes can also be used to investigate how expression of sensory neurons change when the cell cycle is manipulated. As there is much literature to suggest a relationship between the changes in the length of G1 and its effect on neurogenesis, the *ntrk* genes are a valuable tool for better understanding this relationship when studied in a transgenic line of zebrafish with a manipulated cell cycle.

Transgenic lines to manipulate the cell cycle in zebrafish

In order to study the relationship between the cell cycle and differentiation, our lab has two transgenic lines of zebrafish that provide a way to manipulate the cell cycle and observe the effects on development. The first line, *tg(hsp70l:ccnd1DN)* (Figure 4), produces a mutated form of Ccnd1 to force cells into a prolonged G1 phase. Ccnd1 normally binds to Cdk4 to allow progression from G1 into S phase. The dominant negative form of Ccnd1 has T156 and T286 mutated to alanines. The mutations prevent phosphorylation and nuclear export, as well as stabilize the protein to increase half-life (Alt et al., 2000). This line can allow for investigating how manipulating G1 affects the process of zebrafish development.

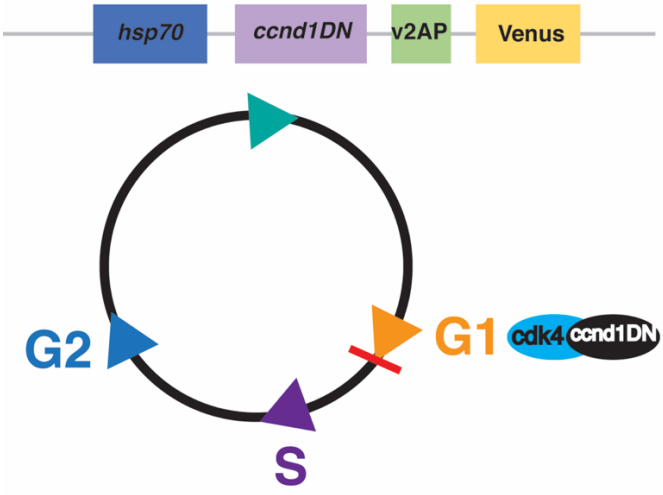

Figure 4. Schematic of the *tg(hsp70l:ccnd1DN)* transgenic line. The *tg(hsp70l:ccnd1DN)* transgenic line contains a heat shock promoter, a mutated form of *ccnd1*, a 2A viral peptide, and the Venus fluorescent protein. Expression of Ccnd1DN causes a prolonged G1 as it takes up endogenous Ccnd1 binding spots but cannot be phosphorylated, preventing cells from moving out of G1 and into synthesis.

In order to confirm that the *tg(hsp70l:ccnd1DN)* construct worked as expected, a previous student quantified the number of cells in G1 after injections with the *tg(hsp70l:ccnd1DN)* construct compared to a control. The constructs were injected into the Dual Fucci line that showed an observable color difference depending on the phase of the cell cycle (Bouldin et al., 2014; Sugiyama et al., 2009) Cells with red nuclei are in G1, while cells with green nuclei are in S/G2/M. As expected, significantly more cells were seen in G1 after injection with the *tg(hsp70l:ccnd1DN)* construct, confirming the line worked as expected (Figure 5).

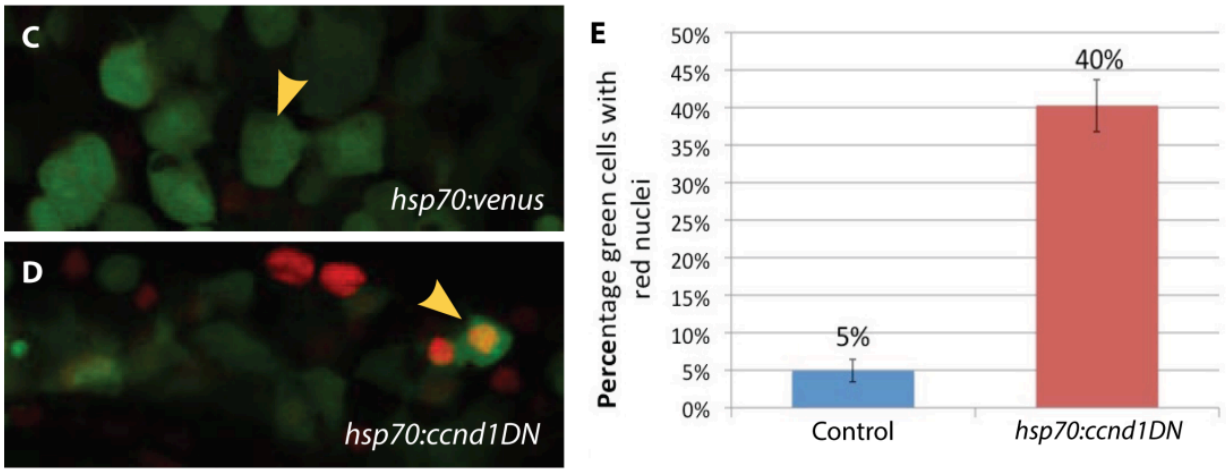

Figure 5. More cells are found in G1 with an *tg(hsp70l:ccnd1DN)* construct. The *tg(hsp70l:ccnd1DN)* transgene has been shown to increase the number of cells found in G1 (n = 196) when compared to a control (n = 202; P < 0.0001). Image taken from Hung, 2015.

The second line, *tg(hsp70l:cdc25)*, expresses *cdc25a* to force cells out of G2 (Figure 6). Neuromesodermal progenitors do not normally express *cdc25a* and these cells have been found to be held in G2 (Bouldin et al., 2014). The transgene contains a mutated form of *cdc25a* with three serine or threonine residues mutated to alanines (*hsp70:*3S/T → A *cdc25a*; referred to as *tg(hsp70l:cdc25)*). The mutated form of Cdc25a, which is expected to have an increased half-life, produced a more severe phenotype than the unmutated form (Bouldin et al., 2014).

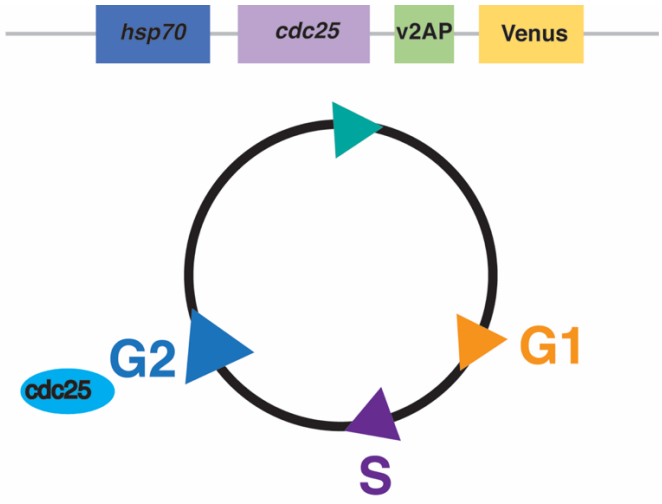

Figure 6. Schematic of the *tg(hsp70l:cdc25)* transgenic line. The *tg(hsp70l:cdc25)* transgenic line contains a heat shock promoter, *cdc25*, a 2A viral peptide, and the Venus fluorescent protein. Expression of this transgene forces cells out of G2 and into mitosis.

Both of these lines contain a heat shock promoter to allow for temporal control of activation. When embryos in either line are subjected to high heat (40 °C), the transgene is activated and the downstream template is transcribed into RNA. This means that transcriptional activation can be controlled temporally. For example, if studying NMP differentiation, a heat shock could be performed at the 15 somite stage, which is when about half of the body segments, or somites, have formed. A heat shock at 15 somites would allow for normal development of half of the body, and the results of the transgene would only be seen in the posterior end that develops after the heat shock. This is especially useful for transgenes that may be lethal or cause severe defects if turned on too early.

In addition to a heat shock promoter, both of these lines contain a viral 2A peptide (v2aP). These are small peptide linker sequences (18-22 amino acids) which are used by some viruses, like the foot-and-mouth disease virus and equine rhinitis A virus, to mediate

protein cleavage (Szymczak et al., 2004). The v2Ap sequence is highly conserved and allows translation of two proteins on either side of the peptide, and then cleavage between a glycine and proline residue by a ribosomal skip mechanism. The glycine and upstream sequence remain as part of protein one and the final proline remains as part of protein two (Liu et al., 2017; Figure 7). Both the *tg(hsp70l:ccnd1DN)* and *tg(hsp70l:cdc25)* transgenic lines have the gene of interest and a fluorescent reporter (Venus) separated by the v2Ap sequence.

Figure 7. The viral 2A peptide sequence can be used for equal expression of multiple proteins. Two genes can be translated from one transcript in equal amounts using a viral 2A peptide via a ribosome skip mechanism (Liu et al., 2017).

The *tg(hsp70l:ccnd1DN)* and *tg(hsp70l:cdc25)* lines each have a distinct phenotype that provides insights into how development is affected. As both lines are under the control of a heat shock promoter, the timing of expression can be tightly controlled. When *tg(hsp70l:ccnd1DN)* embryos were heat shocked at 16.5 hpf and allowed to develop until 72 hpf, a phenotype was observed consisting of a smaller average width and a smaller number of muscle cell nuclei as seen in Figure 8 (Hung, 2015).

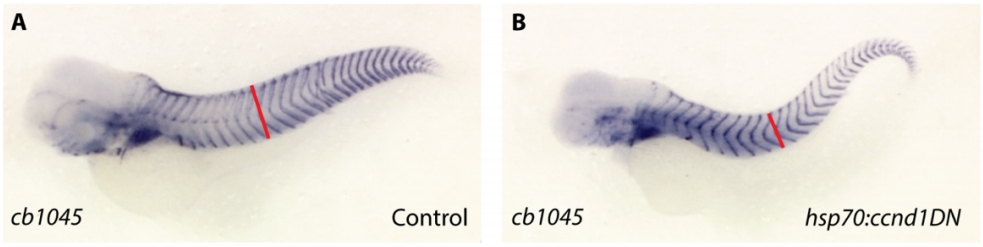

Figure 8. *tg(hsp70l:ccnd1DN)* fish have a characterized phenotype compared to a control. In situ hybridization with cb1045 labels the somite boundaries. Transgenic embryos had a smaller width of their trunk (Hung, 2015).

Because *cdc25* is so carefully regulated in early development, and is not usually expressed by the NMPs that form the posterior body, the *tg(hsp70l:cdc25)* line produces a more severe phenotype than the *tg(hsp70l:ccnd1DN)* line. A phenotypic characteristic of the *tg(hsp70l:cdc25)* line was cell death in the head and eventually throughout the whole body (Bouldin et al., 2014). This cell death is evident by a black area in the head and throughout the body, which obscured the normally be transparent embyro. To mitigate this, a p53 morpholino oligonucleotide (MO) can be co-injected, which allowed for detection of the phenotype specifically associated with the transgene. In previous work with the *tg(hsp70l:cdc25)* line, a heat shock at 12 somites produced shortened embryos with a curved body and an average loss of seven somites (Figure 9; Bouldin et al., 2014).

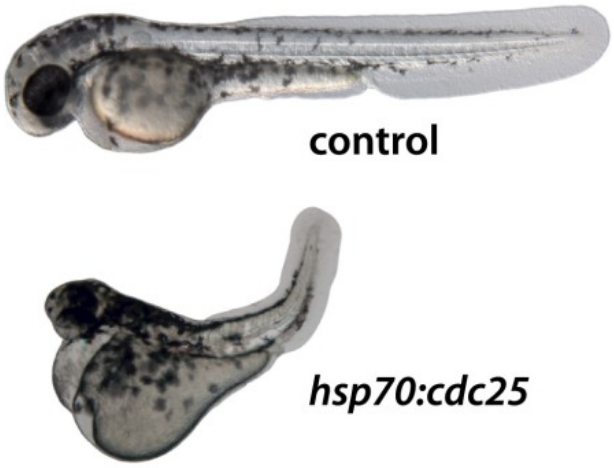

Figure 9. *tg(hsp70l:cdc25)* fish have a characterized phenotype compared to a control. Transgenic organisms show a phenotype of a shorter, curved body with an average loss of seven somites. Image taken from Bouldin et al., 2014.

The *tg(hsp70l:ccnd1DN)* transgenic line provides an important tool for studying the developmental impacts of an extended G1 in vivo. While a significant increase was seen in the number of cells in G1 after activation of the transgene, the number of cells in G1 was

only around 40%. We suspect that this is because this interaction is dependent on where cells are in the cell cycle, and *ccnd1DN* would only have an effect if cells are already in G1 or moving into G1. If a more homogenous population of cells was present, the percentage of cells in G1 would also increase. In addition to using the *tg(hsp70l:cdc25)* line to look at how manipulating G2 affects development, this line can also be used in our investigation of G1. This line forces cells out of G2 and into mitosis, meaning after they divide, cells end up in G1. Because the *tg(hsp70l:ccnd1DN)* line is only effective on cells in G1, crossing these lines together would give a more accurate understanding of how a prolonged G1 is affecting development based on the phenotype seen.

While current and previous work in our lab has used the *tg(hsp70l:ccnd1DN)* line to observe the effects of a prolonged G1 on the development of the vasculature (Phillips, 2017) and neuron specification, understanding the kinetics of this transgene will play an important role in understanding the observed effects. Tissues often have specific critical windows of development, and understanding when and where the transgene is expressed will provide a better understanding how to plan future experiments as well as understanding data already collected. In order to characterize the kinetics of this line, I have used whole-mount RNA in situ hybridization and immunofluorescence to determine location and timing of RNA and protein.

Overall, the present study serves to look at cells specified from NMPs in early development, investigate how the manipulation of G1 affects cell specification by looking at expression of *ntrk* genes, and characterize the kinetics of a transgene used in past, current, and future studies of the Bouldin lab.

MATERIALS AND METHODS

Fish care

Fish were kept between 26-28 °C in a 14 hour light/10 hour dark cycle and were cared for according to *The Zebrafish Book: A guide for the laboratory use of zebrafish (Danio rerio)* (Westerfield, 2000). Water temperature was kept between 26 and 28 °C, conductivity was maintained between 450-650 microSiemens and pH was kept above 6.8. Fish were fed dry food daily at 9 am and live brine shrimp in the afternoon. All zebrafish use was approved by the Appalachian State University Institutional Animal Care and Use Committee (Protocols 17-13 and 17-15).

Embryo collection

Male and female adult zebrafish were separated in breeding tanks in a 2:3 ratio after the afternoon feeding. Breeding tanks contain a larger outer tank and a smaller slightly raised tank to separate embryos from the adult fish as well as a divider to separate the sexes. The next morning the fish were moved to clean water and the dividers were pulled. Fish were given up to 2 hours to breed while checking progress frequently to ensure most embryos would be the same age. Once embryos could be seen at the bottom of the tank, adult fish were removed from the breeding tank. Embryos were poured through a mesh filter to collect and rinsed with RO water into a glass petri dish. Fertilized, live embryos were then moved to embryo media (15 mM NaCl, 0.8 mM KCl, 1.3 mM $CaCl \bullet 2H_2O$, 0.1 mM KH_2PO_4, 0.05 mM Na_2HPO_4, 2 mM $MgSO_4 \bullet 7H_2O$, 0.07 mM $NaHCO_3$) and put in a 28 °C incubator.

Embryo staging

Embryos were staged according to *Stages of embryonic development of the zebrafish* (Kimmel et al., 1995). Bud stage embryos are 10 hpf and are recognized by the swelling of the posterior end, known as the tailbud. Embryos at the 15 somite stage can be easily distinguished by the number of somites present, as well as by yolk extension length. By Prim-5 stage or 24 hpf, embryos have about 30 somites, have developed faint melanin pigment, and have a distinct angle between the head and trunk. Visual cues and somite numbers were used to accurately determine staging throughout embryogenesis.

Heat shock to induce transgene expression

Embryos were collected from a cross and kept in a glass petri dish at a temperature of 16-30 °C until the intended heat shock time point. If embryos were kept at a temperature below 28 °C, embryos were moved to 28 °C prior to heatshock. 30 mL of embryo media was heated in a water bath at 40 °C for at least 30 minutes prior to heat shock. Embryos were transferred to a 50 mL conical tube and any excess embryo media was removed. The heated embryo media was then poured into the conical tube containing the embryos and embryos were left in the water bath for 30 minutes. After 30 minutes embryos and the 30 mL of embryo media were poured into a clean petri dish. After 2 hours, embryos could be sorted as transgenic or non-transgenic siblings using fluorescence and placed in separate dishes.

Embryo fixation

Embryos were fixed for in situ hybridization at specific developmental stages determined based on the gene of interest. All embryos were collected from crosses (either wildtype embryos from a wildtype cross, or transgenic embryos from a *tg(hsp70l:ccnd1DN)* x wildtype cross) and kept at 22-28 °C until the time points of interest. Wildtype embryos used for in situ hybridization were fixed at time points of 16.5 hpf and 24 hpf. For 24 hpf embryos, 1-phenyl 2-thiourea (PTU) was added to embryo media prior to 24 hpf to prevent melanin production. *tg(hsp70l:ccnd1DN)* embryos were heat shocked at bud stage for use with the Venus probe and 16.5 hpf for use with the *ntrk2a* probe. Two hours after the heat shock was performed embryos were sorted by fluorescence as transgenic or non-transgenic and fixed at time points of 2, 4, 6 h post heat shock (h pHS) for the Venus probe or 24 hpf for *ntrk2a*. All embryos were fixed in 4% paraformaldehyde overnight and dehydrated stepwise into methanol for storage.

Phylogenetic tree construction

A phylogenetic tree was generated using Phylogeny.fr (http://www.phylogeny.fr/). Trk receptor sequences of six vertebrate species (*D. rerio*, *X. tropicalis*, *G. gallus*, *M. musculus*, *R. norvegicus*, and *H. sapiens*) were retrieved from NCBI (Table I).

Table I. Accession numbers of *NTRK* genes used to construct a phylogenetic tree.

Organism	Gene	Accession Number
D. melanogaster	*off-track*	NP_523705.2
D. rerio	*ntrk1*	NP_001288285.1
	ntrk2a	XP_009302567.1
	ntrk2b	NP_001184090.2
	ntrk3a	NP_001243593.1
	ntrk3b	XP_017212461.1
H. sapiens	*NTRK1*	NP_001007793.1
	NTRK2	NP_001007098.1
	NTRK3	NP_001007157.1
M. musculus	*Ntrk1*	XP_006501187.1
	Ntrk2	NP_001020245.1
	Ntrk3	NP_032772.3
R. norvegicus	*Ntrk1*	NP_067600.1
	Ntrk2	NP_001156640.1
	Ntrk3	NP_001257584.1
X. tropicalis	*ntrk1*	XP_002939035.1
	ntrk2	NP_001072653.1
	ntrk3	XP_004912706.1
G. gallus	*NTRK1*	NP_990709.1
	NTRK2	NP_990562.1
	NTRK3	NP_990500.1

Sequences were aligned using MUSCLE alignment 3.8.31 with find diagonals option disabled and maximum number of iterations set at 16. The alignment was refined using Gblocks 0.91b to remove alignment noise. Settings include: the minimum number of sequences for a conserved position was set at half the number of sequences +1, the minimum number of sequences for flank position was set at 85% of the number of sequences, maximum number of contiguous nonconserved positions was set to 8, the minimum length of a block was set to 10, and the allowed gap positions was set to none. Phylogeny used PhyML3.1/3.0 alRT and was set to 4 substitution rate categories, estimated gamma parameter, estimated proportion of invariable sites, and a transition/transversion ratio of 4. The tree rendering was done with TreeDyn 198.3.

Probe synthesis

RNA probes were synthesized with 10 µg of plasmid DNA. Plasmid DNA was linearized using restriction digest and then linearized DNA was extracted by a phenol/chloroform extraction. DNA was resuspended in water and used in a transcription reaction. The transcription reaction contained 2 µl 10x RNA polymerase buffer, 2 µl 10x DIG labeling mix (Roche), 1-2 µg of linearized DNA template, 1 µl of RNAsin (Invitrogen), 2 µl of T7 or T3 polymerase (New England Biolabs), and water up to 20 µl. This reaction was left at 37 °C for 2 hours and then 2 µl of DNAse was added for 30 minutes. 30 µl of water and 25 µl of LiCl solution was added and the sample was incubated at -20 °C for 30 minutes. A 15 minute spin was done at 4 °C followed by an ethanol wash. For non-hydrolyzed probes (*ntrk2a, ntrk3a, Venus)* the pellet was resuspended in water and hybridization buffer was added. For hydrolyzed probes (*ntrk1, ntrk2b, ntrk3b)*, the pellet was

resuspended in water and then hydrolyzed with sodium bicarbonate and sodium carbonate. Hydrolysis occurred by adding 5 µl 0.4 M $NaHCO_3$ and 5 µl 0.6 M Na_2CO_3 and incubating at 60 °C for t minutes where t = (starting kb - desired kb) / 0.11* (starting kb) (desired kb) with 0.35 kb used as desired size. Hydrolyzed probes were cleaned up with Macherey-Nagel NucleoSpin RNA Clean-up kit.

In situ hybridization

Single-probe whole-mount in situ hybridization was performed with embryos previously dehydrated in methanol. Embryos were rehydrated using a 50% MeOH/50% PBT (phosphate-buffered saline with Tween 20) mixture and then washed two times with PBT. A proteinase K digestion was done at a concentration of 2 µg/mL for 5 minutes for 15 somite embryos or 17 minutes for 24 hpf embryos. After proteinase K, the embryos were fixed again in 4% paraformaldehyde (PFA) and then washed two times with PBT. PBT was removed and hybridization mix (hyb-) was added for 2-5 hours at 65 °C. The hyb- was removed and a 1:200 dilution of the probe in hybridization mix (hyb+) was added to embryos and incubated at 65 °C overnight. The RNA probe was removed and the following washes were done: 1 minute in hyb-; 45 minutes in 50% hyb-/50% 2X SSC; 15 minutes 2X SSC; 60 minutes 0.2X SSC; and then three 5 minute PBT washes. The embryos were blocked using 2% goat serum and 2 mg/mL BSA in PBT for 3 hours at 4 °C. The block was removed. Then, a solution of block plus anti-DIG antibody fragments was added to embryos and left overnight at 4 °C. The following day six 15 minute PBT washes. Then, three 5 minute washes in alkaline phosphatase buffer were performed. The embryos were then left to develop in a solution of

alkaline phosphatase buffer plus BCIP/NBT and left until color change was seen. The reaction was stopped with PBT and then dehydrated back into methanol.

Immunofluorescence

Embryos were collected from a *tg(hsp70l:ccnd1DN)* x wildtype cross and heat shocked at 16.5 hpf. Embryos were screened for fluorescence and separated into transgenic and non-transgenic siblings and then fixed at 3, 6, and 9 h pHS in 4% PFA overnight. Embryos were dehydrated into methanol for storage and rehydrated into PBST before use. Rehydrated embryos were permeabilized with 2 µg/mL of proteinase K for 8 minutes (3 h pHS embryos), 10 minutes (6 h pHS), and 14 minutes (9 h pHS) and then re-fixed in PFA. Embryos were incubated in fish block for 2 hours at RT and then incubated in v2Ap 1° antibody (1:200 in fish block, Novus, #NBP2-59627SS) overnight at 4°C. The following day, embryos were washed in PBST for 60-90 minutes with 4-6 changes of buffer and incubated in the 2° antibody (1:1000, rabbit anti-mouse Alexa Fluor555, Thermo # A-21427) and left overnight at 4°C. The 2° antibody was discarded and embryos were re-fixed in PFA, washed with PBST, and then moved stepwise to a solution of 75% glycerol and 25% PBS and left overnight.

Microscopy and image collection

To screen transgenic organisms and separate transgenic from non-transgenic siblings, a Meiji Techno EMZ-8TRD microscope was used with a NIGHTSEA cyan light filter. After transgenic and non-transgenic organisms had been identified and fixed, all embryos were moved stepwise to a solution of 75% glycerol and 25% PBS and left overnight. The

following day embryos were mounted on a 1.0 mm thick Gold Seal slide and covered with a Corning 22 x 22 mm cover slip. All embryos were imaged on an Olympus IX81 at 4x or 10x magnification and processed on Olympus cellSens software.

Cell Counting

ImageJ was used to determine cell counts of *tg(hsp70l:ccnd1DN)* embryos after in situ hybridization with *ntrk2a* probe. A 1 mm line was drawn in ImageJ from the midbrain-hindbrain boundary down the length of the embryo, where another line was drawn. Cells in between the midbrain-hindbrain boundary and the second line (1 mm distance) were counted using the ImageJ cell counter and recorded in Microsoft Excel. Each count was done three times and the average of the counts were taken. A p-value was determined using the two-tailed t-test function in Excel.

Fin clip & DNA extraction

In order to obtain DNA for genotyping, DNA was extracted from the tip of the caudal fin. To do this, adult fish were anesthetized in cold water until movement had ceased, and then sterile scissors were used to clip the tip of the caudal fin and the fin was moved to a sterile tube. Fish were moved to fresh 28 °C water and watched to confirm their recovery. Any excess water was removed from the tube containing the fin, and genomic extraction buffer (10 mM Tris pH 8.2, 10 mM EDTA, 200 mM NaCl, 0.5% SDS, and 200 mg/mL proteinase K) was added. Tubes were placed on a shaker at 56 °C and 100 rpm for 3 hours or until the fin had completely dissolved. Next, 100 ml of 100% ethanol was added and the

samples were incubated at -20 °C overnight. The following day, samples were spun at 13000 rpm for 10 minutes and the supernatant was removed. Then, 200 mL of 70% ethanol was added and the samples were spun at 13000 rpm for 2 minutes and the supernatant was removed and the pellet was allowed to dry. Next, a solution of TE+RNase was added (10mM Tris, 1 mM EDTA pH 8.0, 100 mg/mL RNAse) and the solution was incubated for 1 hour at 37 °C. The volume was matched with a 50% phenol/50% chloroform solution and spun for five minutes at full speed. The supernatant was removed, 50% phenol/50% chloroform was added and spun again for five minutes. The supernatant was moved to a fresh tube DNA and precipitated with 2.5 volumes of 100% ethanol and 5 M NaCl to bring the final concentration to 0.2 M NaCl. The samples were incubated at -20 °C overnight. The next day, the samples were spun at 4 °C for 30 minutes and the supernatant was removed. Then 500 ml of 70% ethanol was added, and the samples were spun for 10 minutes. The supernatant was removed and after the pellet dried, the samples were resuspended in water.

To genotype single embryos, the fin clip DNA extraction was followed with a single embryo in a tube instead of the caudal fin.

Genotyping

After DNA was extracted, PCR was performed for genotyping transgenic fish using primers found in Table II, which amplify a 300 bp section of the transgene.

Table II. Genotyping primers used for confirmation of *tg(hsp70l:ccnd1DN)* and *tg(hsp70l:cdc25a)* lines.

Primer Name	Sequence
hsp70cdc25 primer 1	TAGAGTGTCCCAGTCCTTT
hsp70cdc25 primer 2	CATGGAGGGCTTTTTGAACT
hsp70ccdn1DN primer 1	CAGACAATGCTTAAAGCTGA
hsp70ccnd1DN primer 2	AGCCAGAAACATACAAGTTG

Genotyping PCR

Approximately 200 ng was used in a polymerase chain reaction to test genotyping primers (Table I). A 25 µl reaction was prepared to contain template DNA, 2.5 µl 10x Taq buffer, 1.25 µl of each forward and reverse primers, 0.5 µl dNTPs, 0.25 µl Taq (GenScript), and water up to volume. Thermal cycler settings were as follows: initial denaturation at 94 °C for 30 s, 35 cycles of 94 °C for 10 s, 55 °C for 30 s, and 72 °C for 30 s, with a final extension of 7 minutes at 72 °C.

Cloning: Moving tagRFP from PCRII vector to Tol2 vector containing *cdc25* gene

Approximately 250 ng of PCRII.TagRFP DNA was used in a polymerase chain reaction to amplify TagRFP with an added *SalI* cut site. A 25 µl reaction was prepared to contain template DNA, 5 µl of 5x Phusion High Fidelity buffer, 1.25 µl of each forward and reverse primers, 0.5 µl of dNTPs, 0.25 µl of Phusion polymerase (Thermo Scientific), and water up to volume. Thermocycler settings were as follows: initial denaturation at 98 °C for 60 s, 35 cycles of 98 °C for 10 s, 60.5 °C for 30 s, and 72 °C for 60 s, with a final extension of 10 minutes at 72 °C.

Table III. Primers used to amplify TagRFP and add *SalI* cut site.

Primer Name	Sequence
TagRFP forward	GCGTCGACATGGTGTCTAAGGGCGAA
TagRFP reverse	CACTATAGGGCGAATTGGG

QuikChange site-directed mutagenesis

25-100 ng of the pBluescript.*cdc25* plasmid was used in a QuikChange (®, Agilent) site-directed mutagenesis to mutate an *XhoI* cut site to *PstI* (primers found in Table III). A 25 µl reaction was prepared to contain template DNA, 5 µl of 5x Q5 or Phusion high fidelity buffer, 1.25 µl of each forward and reverse primers, 0.5 µl of dNTPs, 0.25 µl of Q5 (NEB) or Phusion (Thermo Scientific) polymerase, and water up to volume. Thermal cycler settings were as follows: initial denaturation at 98 °C for 2 minutes, 17 cycles of 98 °C for 15 s, 60 °C for 30 s, and 72 °C for 5 minutes, with a final extension of 5 minutes at 72 °C. After

samples were removed from the thermal cycler, 5 µl of each reaction was moved to a new tube and 0.5 µl of *DpnI* was added. Samples were incubated at 37 °C for 3 hours and then run on a gel for analysis.

Table IV. Primers used for QuikChange site-directed mutagenesis.

Primer Name	**Sequence**
XhoI to PstI	ACGAGCTGTACAAGTAACTGCAGCCTCTAGAACTATAGTG
TagRFP reverse	CACTATAGTTCTAGAGGCTGCAGTTACTTGTACAGCTCGT

Protein extraction for Western blots

Embryos were transferred to a microcentrifuge tube containing 1 ml of deyolking buffer (55 mM NaCl, 1.8 mM KCl, and 1.25 mM $NaHCO_3$) at 3, 6, and 9 h pHS. Embryos were mixed for 5 min at 1100 rpm to dissolve yolk and then spun at 2100 rpm for 30 seconds. The supernatant was discarded and 0.27 µl of Rubinfeld's lysis buffer (20 mM Tris pH 8, 140 mM NaCl, 1% Triton X-100, 10% glycerol, 1 mM EGTA, 1.5 mM $MgCl_2$, 1 mM Na_3VO_4, and 50 mM NaF; Rubinfeld et al., 1993) was added. Embryos were homogenized with pestle and spun at full speed for 15 minutes at 4 °C. Lysate was removed and frozen for western blotting.

Western blotting

Protein was diluted 1:1 with 2X Laemmli buffer (4% SDS, 20% glycerol, 0.120 M Tris pH 6.8, 0.02% bromphenol blue, 5% 2-Mercaptoethanol) and denatured at 80 °C for 5 minutes. Samples were run on 4-20% gradient polyacrylamide gel at 200 V for approximately 45 minutes. Gel, nitrocellulose membrane, and blotting paper were equilibrated in 1X transfer buffer (Bio rad 10x Tris/Glycine buffer) for 5 minutes. Air bubbles were removed and proteins were transferred to a nitrocellulose membrane at 100 V for 1 hour. The membrane was blocked with 5% skim milk in PBT for 1 hour at RT followed by 3 room temperature PBT washes at 5 minutes each. Then the membrane was incubated in primary v2Ap antibody (Novus) overnight at 4 °C. PBT washes were repeated and the membrane was incubated in secondary antibody (GAM-HRP) for 1 hour at room temperature. PBT washes were repeated followed by addition of ECL reaction mix (Thermo Scientific). The membrane and ECL mix was left in the dark for 5 minutes and then imaged.

RESULTS

Neuromesodermal progenitors (NMPs) are bipotential cells that can give rise to mesoderm or ectoderm to contribute to the elongating body of a zebrafish embryo (Kondoh and Takemoto, 2012). NMPs are located in the tailbud and are needed to form the somites, notochord, sensory neurons, and spinal cord of the posterior body during embryogenesis. The specification of sensory neurons in early development is critical for survival, as these neurons allow an organism to sense their environment. The specific functionality of *ntrk* genes in zebrafish is not fully understood and learning the genetic similarities between the zebrafish genes and the genes in other species, as well as determining patterns of expression, will help provide a better understanding of the *ntrk* genes and their function.

ntrk expression in embryonic zebrafish

Expression of genes in the *ntrk* family is one way of looking at specification of sensory neurons during early development of zebrafish. Expression of *ntrk* genes is required for survival of specific subsets of somatosensory neurons (Huang and Reichardt, 2001), making *ntrk* genes a useful marker of these neurons in vivo. Because zebrafish have five *ntrk* genes, instead of the three found in most vertebrates, including the paralogs *ntrk2a/ntrk2b*, and *ntrk3a*/*ntrk3b*, a phylogenetic tree was generated to determine which paralogs were most closely related to *ntrk* genes in other species (Figure 10). Because these are protein coding genes, amino acid sequences were used to generate the tree. All sequences were acquired from NCBI (Table I). The *ntrk* genes in zebrafish were compared to *H. sapiens*, *R.*

norvegicus, *M. musculus*, *G. gallus*, and *X. tropicalis*. *D. melanogaster* off-track and off-track 2 sequences were used to root the tree as these are receptor tyrosine kinases in a non-vertebrate species. From the phylogenetic tree it was determined that *ntkr2a* is most closely related to *Ntrk2* in other species, and *ntrk3a* is most closely related to *Ntrk3* in other species.

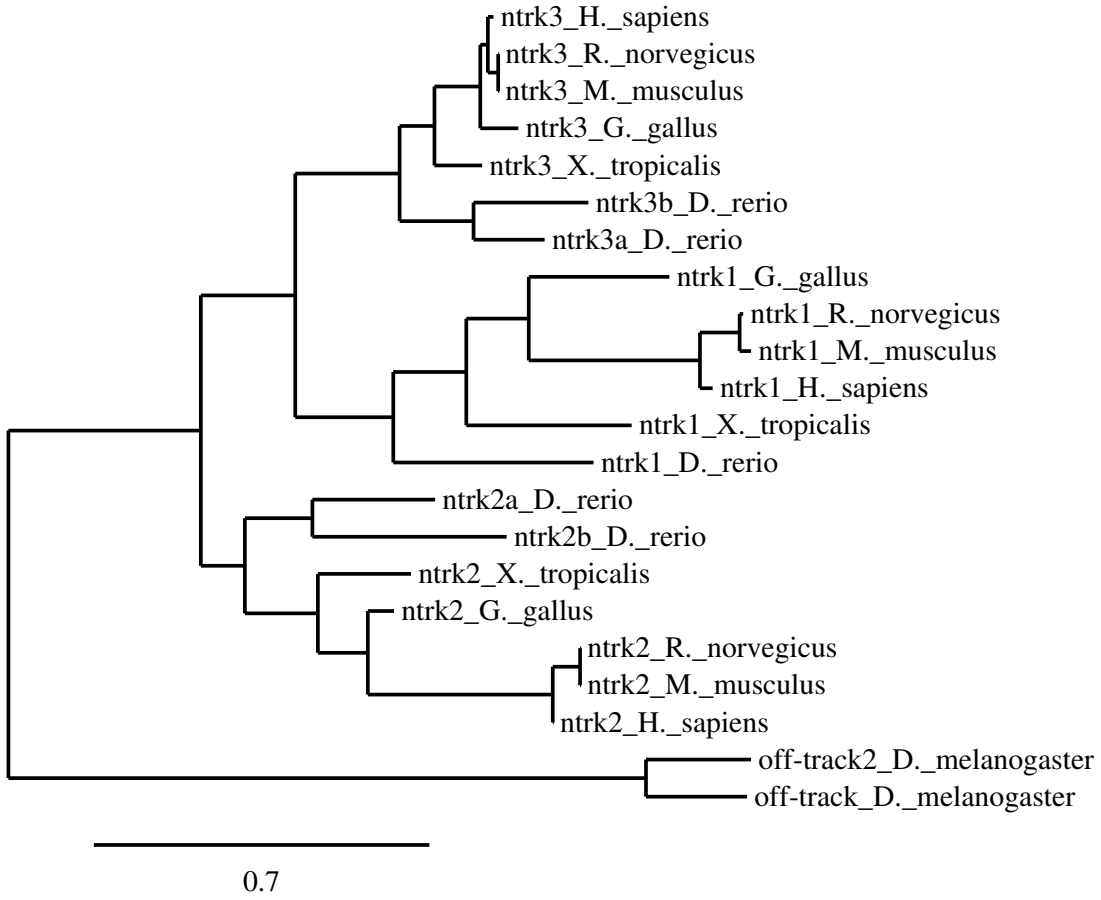

Figure 10. Phylogenetic tree comparing *ntrk* genes in *D. rerio* to other species. The Trk receptor amino acid sequences of six species was compared to determine the zebrafish paralogs that are most closely related to other species.

Once phylogeny had been determined, zebrafish *ntrk* gene expression was determined at two points in early development, 16.5 hpf and 24 hpf, using whole mount in situ hybridization. 16.5 hpf was chosen because at this time embryos are undergoing embryonic patterning and neurons are first being specified. By 24 hpf, embryos have undergone

embryonic patterning and sensory motor reflexes are beginning (Kimmel et al., 1995), making these useful time points to look at early specification of neurons.

In zebrafish, only one *ntrk1* gene is present. Expression of the *Ntrk1* gene in mice causes survival of nociceptors, the sensory neurons responsible for detecting potentially harmful stimuli (Purves et al., 2001). The *ntrk1* gene in zebrafish has been assumed to share function with *Ntrk1* in mice. *ntrk1* expression has not been previously determined by other studies at 16.5 hpf, but has been seen in cranial neurons, trigeminal ganglia, and Rohon-Beard (RB) neurons at 24 hpf (Nittoli et al., 2018). While previous studies have used partial gene sequences for making probes, the current study used full length sequences that were hydrolyzed into 300-400 bp fragments. A hydrolyzed full-length probe means that binding should not favor any specific region or splice isoform. Using the *ntrk1* probe, expression was found at 16.5 hpf in two sets of cranial ganglia and at 24 hpf in two sets of cranial ganglia as well as Rohon-Beard neurons of the spinal cord (Figure 11).

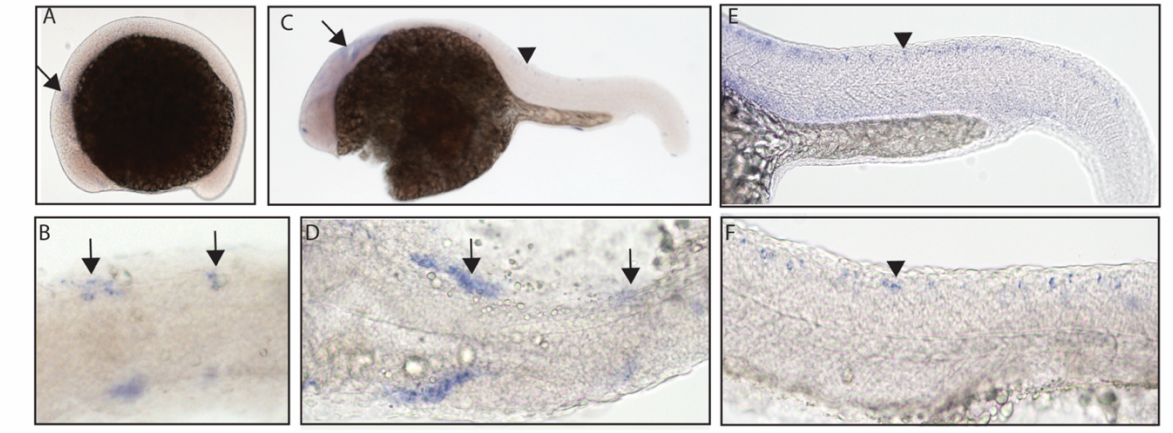

Figure 11. Early expression of *ntrk1* is seen in the head and spinal cord using whole-mount RNA in situ hybridization at 16.5 hpf and 24 hpf. All embryos oriented with head to the left in lateral view (a, c, e, f) and dorsal view (b, d). Expression at 16.5 hpf (a,b) was seen in two sets of cranial ganglia (arrow). At 24 hpf (c-f), expression was seen in two sets of cranial ganglia (arrow) as well as Rohon-Beard neurons (arrowhead). This data is representative of three rounds of in situ hybridization with at least 25 embryos per round.

Zebrafish have two paralogs of the *Ntrk2* gene, *ntrk2a* and *ntrk2b.* Because *ntrk2a* is most closely related to *Ntrk2* in other species, these genes were assumed to be functionally similar. Previous studies have determined expression of *ntrk2a* in the trigeminal ganglia and RB neurons as early as 24 hpf (Martin et al., 1995; Nittoli et al., 2018). The current study confirms expression in the trigeminal ganglia and RB neurons as early as 16.5 hpf as well as in the trigeminal ganglia and RB neurons at 24 hpf (Figure 12).

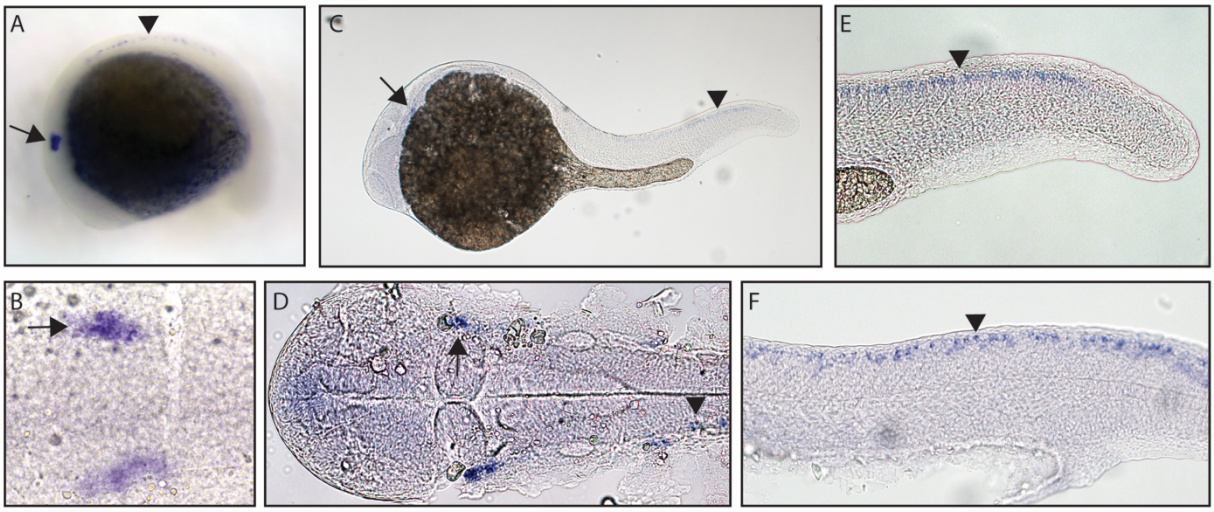

Figure 12. Early expression of *ntrk2a* is seen in the head and spinal cord using whole-mount RNA in situ hybridization at 16.5 and 24 hpf. All embryos oriented with head to the left in lateral view (a, c, e, f) and dorsal view (b, d). Expression at both 16.5 hpf (a,b) and 24 hpf (c-f) was seen in trigeminal ganglia (arrow) as well as Rohon-Beard neurons in the spinal cord (arrowhead). This data is representative of two rounds of in situs with at least 25 embryos per round.

The function of *ntrk2b* is unknown, and the expression is distinct from that of *ntrk2a*. Other studies using partial sequence probes suggest that expression is found in the telencephalon, thalamus, hypothalamus, tegmentum, hindbrain, cranial nerves, and RB neurons (Nittoli et al, 2018). Using a full-length hydrolyzed probe, no expression of *ntrk2b* was seen at 16.5 hpf, and expression at 24 hpf was seen in the telencephalon (Figure 13).

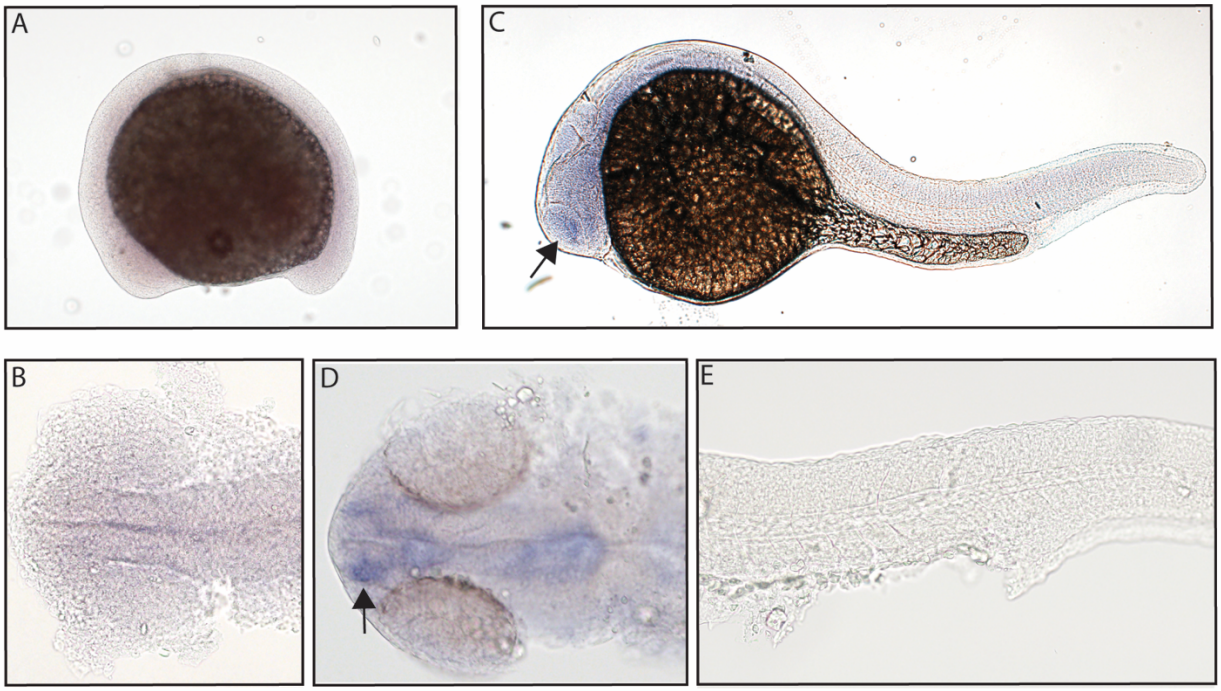

Figure 13. Early expression of *ntrk2b* is seen in the head using whole-mount RNA in situ hybridization at 16.5 and 24 hpf. All embryos oriented with head to the left in lateral view (a, c, e) and dorsal view (b, d). No expression was seen at 16.5 hpf (a,b). Expression was seen at 24 hpf (c-e) in the telencephalon (arrow). This data is representative of three rounds of in situ hybridization with at least 25 embryos per round.

Zebrafish have two paralogs of the *Ntrk3* gene, *ntrk3a* and *ntrk3b. ntrk3a* has been assumed to be most functionally similar to *Ntrk3* in other species as it is the most closely related. Previous studies have determined expression of *ntrk3a* in the telencephalon, pineal gland, hypothalamus, cranial ganglia, and RB neurons at 24 hpf (Nittoli et al., 2018). The current study confirms expression in the telencephalon and RB neurons at 24 hpf and finds no expression detected at 16.5 hpf (Figure 14).

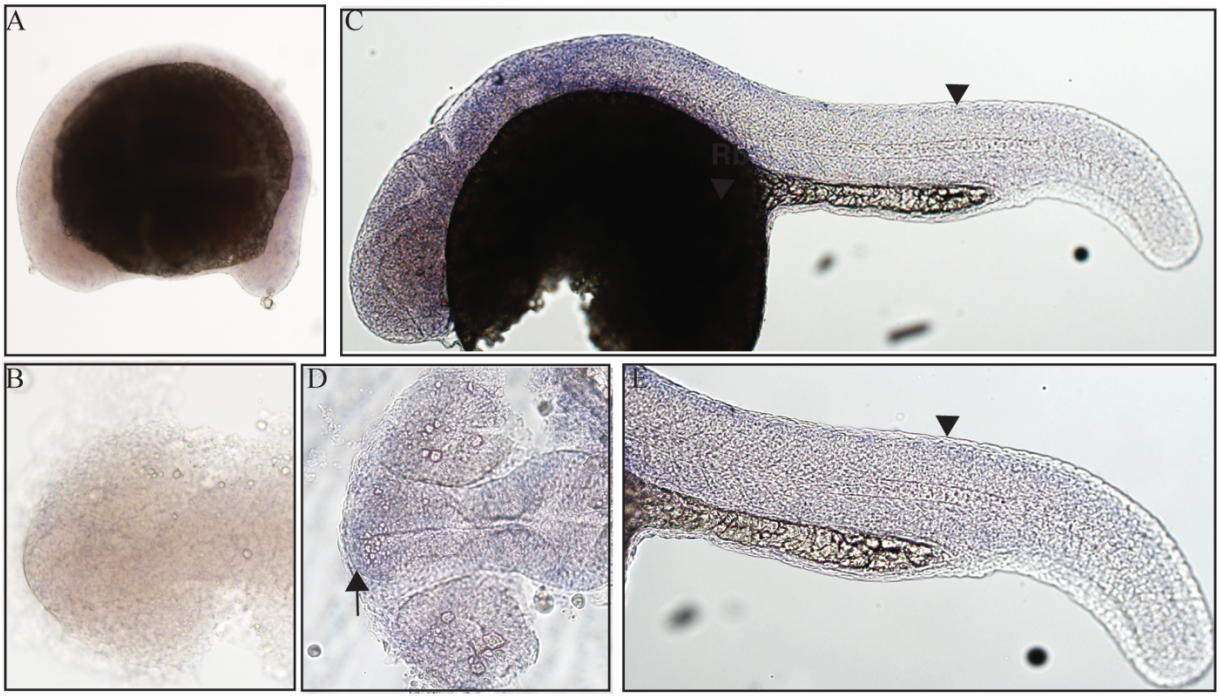

Figure 14. Early expression of *ntrk3a* is seen in the head and spinal cord using whole-mount RNA in situ hybridization at 24 hpf. All embryos oriented with head to the left in lateral view (b, c, e) and dorsal view (a, d). No expression was seen at 16.5 hpf (a,b). Expression was seen at 24 hpf (c-e) in the telencephalon (arrow) and spinal cord (arrowhead). This data is representative of three rounds of in situ hybridization with at least 25 embryos per round.

The function of *ntrk3b* is unknown, and there is some overlap in expression with *ntrk3a*. Other studies using partial sequence probes suggest that expression is found in the telencephalon, thalamus, tegmentum, and otic vesicle at 24 hpf (Nittoli et al, 2018). Using a full-length probe, the present study confirms expression in the telencephalon and otic vesicle and identified expression in the midbrain and hindbrain at 24 hpf (Figure 15).

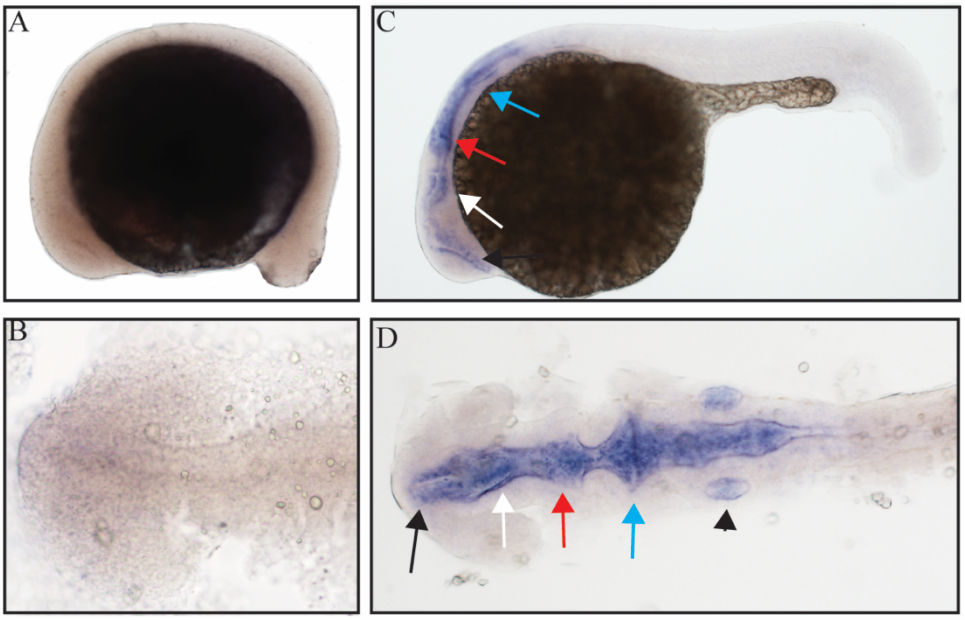

Figure 15. Early expression of *ntrk3b* is seen throughout the head at 24 hpf using whole-mount RNA in situ hybridization. Expression was seen in the telencephalon (black arrow), midbrain (white arrow), hindbrain (red arrow), lateral line primordium (blue arrow), and otic vesicle (black arrowhead) at 24 hpf (c, d) with no expression detected at 16.5 hpf (a, b). All embryos oriented with head to the left in lateral view (a, c) and dorsal view (b, d). This data is representative of three rounds of in situ hybridization with at least 25 embryos per round.

p75 NTR is known to bind with low affinity to each of the neurotrophins that bind the Trk receptors (Meeker and Williams, 2015). No specific *p75* expression was detected at 16.5 hpf with diffuse staining observed throughout the embryo. By 24 hpf, expression can be seen in two sets of cranial ganglia (Figure 16).

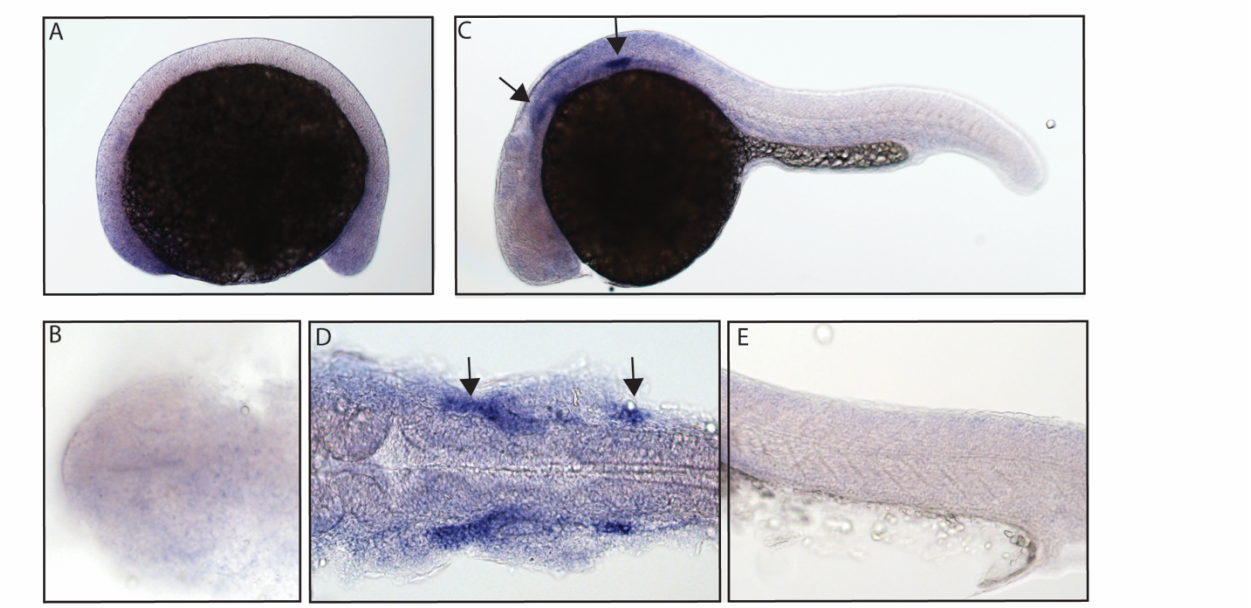

Figure 16. Early expression of *p75* NTR is seen at 24 hpf in two sets of cranial ganglia. All embryos oriented with head to the left in lateral view (a, c, e) and dorsal view (b, d). No expression was seen at 16.5 hpf (a,b). Expression was seen at 24 hpf (c-e) in the two sets of cranial ganglia (arrow). This data is representative of two rounds of in situ hybridization with at least 25 embryos per round.

Examining differences in *ntrk2a* expression in *tg(hsp70l:ccnd1DN)* embryos

In order to explore the relationship between the length of G1 and specification of neurons during early zebrafish development, expression of the *ntrk2a* gene was compared between wildtype and *tg(hsp70l:ccnd1DN)* transgenic embryos (Figure 17). The *tg(hsp70l:ccnd1DN)* line produces a mutated form of *ccnd1* that is presumed to bind to Cdk4, but is unable to be phosphorylated, making the cells unable to move into synthesis (Hung, 2015). This line provides a way to manipulate G1 and determine how development is affected, like with the expression of sensory neurons in early development.

ntrk genes can be used as a marker of terminally differentiated sensory neurons. To look at changes in expression, *ntrk2a* was chosen first, because it is the only *ntrk* gene

determined to be expressed in the spinal cord at 16.5 hpf, providing a way to look at early specification of NMPs into spinal cord neurons, and second, it produced the most robust and reliable staining. Embryos were sorted as transgenic or non-transgenic siblings using fluorescence, heat shocked at 16.5 hpf, and fixed at 24 hpf. In situ hybridization was performed using the *ntrk2a* probe on embryos collected from a *tg(hsp70l:ccnd1DN)* x wildtype cross. Cells in a 1 mm portion of the embryo starting from the midbrain-hindbrain boundary (MHB) were counted to determine if a difference in expression could be seen. Overall, no significant difference was seen in the number of puncta between transgenic and non-transgenic siblings (Table V; $p = 0.24$).

Table V. Cell counts* for *ntrk2a* expression in *ccnd1DN* and wildtype embryos.

Embryo	**1**	**2**	**3**	**4**	**5**	**6**	**7**	**8**	**9**	**10**	**Average**
Wildtype	52	43	48	50	36	40	37	42	39	40	42.7
ccnd1DN	45	38	40	47	30	39	45	30	48	44	40.6

*Each cell count value is the average of three rounds of counting.

While no significant quantitative differences were noted, qualitative differences were observed. The first difference is the overall color of the embryo after in situ hybridization was performed. While both sets of embryos were treated with the same dilution of probe for the same time and the color was developed for the same time, all ten of the transgenic embryos were noted as being darker in color, with what appeared to be diffuse staining throughout the embryo. In addition, the size of the puncta appeared different between the transgenic and non-transgenic embryos. Wildtype embryos had larger, more easily countable puncta while *ccnd1DN* embryos had qualitatively smaller puncta that were harder to count (Figure 17).

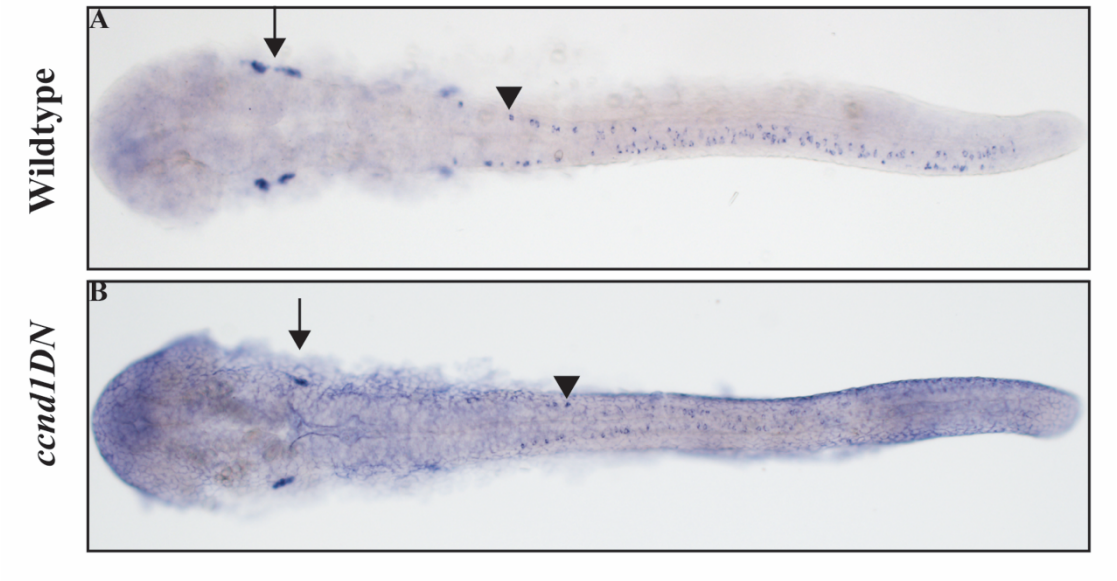

Figure 17. Whole-mount in situ hybridization was used to determine differences in *ntrk2a* expression between wildtype (A) and *ccnd1DN* (B) embryos. Expression can be seen in both cranial ganglia (two domains seen in wildtype, one in *ccnd1DN*; indicated by arrow), and in Rohon-Beard neurons along the spinal cord (indicated by arrowhead).

A more quantitative difference was noted in the expression pattern seen in the cranial ganglia, which are a population of neurons that are not expected to be derived from neuromesodermal progenitors. Half (5/10) of the wildtype embryos showed two domains of cranial ganglia staining on both sides of the MHB, while this was seen in none of the transgenic embryos. Another pattern noted was asymmetric expression in the cranial ganglia, with the left and right side of the head having a different number of expression domains. One transgenic embryo showed this pattern, with two domains of cranial ganglia expression on one side of the MHB and one domain on the other side. This pattern was also seen in two wildtype embryos. Most (9/10) of the transgenic embryos showed one domain of cranial ganglia staining on each side of the MHB which was seen in three of the wildtype embryos. The nine transgenic embryos that showed one domain of cranial ganglia on both sides of the

MHB were categorized into either one domain of staining that was the equivalent to the domain of staining seen in wildtype (large), or one domain of staining that appeared approximately half the size as the domain of staining seen in wildtype (small). Of the nine, three embryos fit into the category of one large domain, while six embryos showed only one small domain of cranial ganglia staining on both sides of the MHB that appeared to be half the size of the domain of staining seen in wildtype embryos (Figure 18).

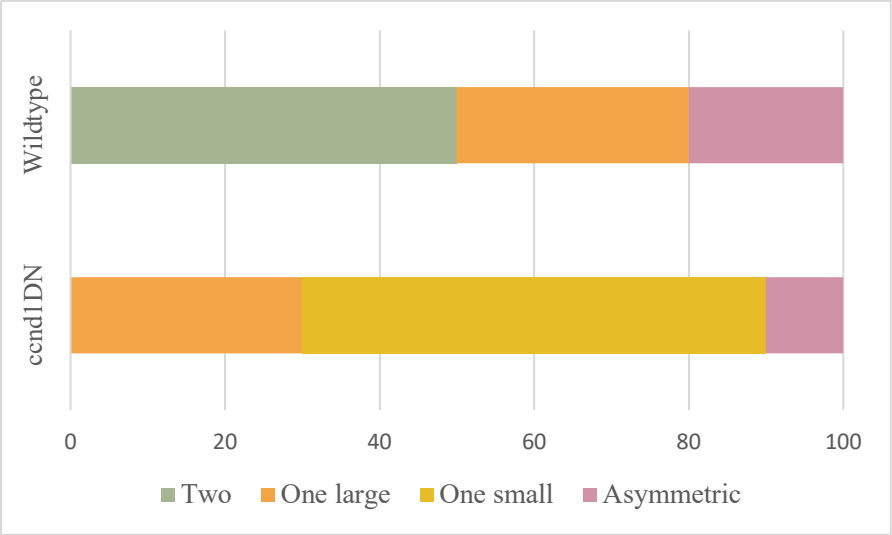

Figure 18. *ntrk2a* expression patterns observed in the cranial ganglia. Ten *ccnd1DN* embryos and ten wildtype embryos were categorized into one of four categories based on the observed cranial ganglia staining pattern. Embryos were categorized as having two domains of staining, one large domain of staining, one small domain of staining, or asymmetric staining.

Characterizing the kinetics of the *tg(hsp70l:ccnd1DN)* transgenic line

The *tg(hsp70l:ccnd1DN)* transgenic line of zebrafish uses a mutated version of *ccnd1DN* to prolong the time cells spend in G1. The working order of this transgene was confirmed by a previous student who determined that when embryos were injected with the *tg(hsp70l:ccnd1DN)* construct, significantly more cells were in G1 compared to cells with

the construct minus the *ccnd1DN* sequence (Figure 5). This construct was used to make a stable transgenic line that allows our lab to study the effects of a prolonged G1 on embryonic development. In order to better plan experiments with this line, like determining how *ntrk2a* expression changes with a prolonged G1, I determined the kinetics of the transgene by looking at timing and location of both RNA and protein.

Embryos from a *tg(hsp70l:ccnd1DN)* x wildtype cross were collected and heat shocked at bud stage (10 hpf). Embryos were sorted according to fluorescence as transgenic or non-transgenic siblings and then fixed at 2, 4, and 6 hours post heat shock (h pHS). Whole-mount RNA in situ hybridization was performed using a probe that is complementary to the viral 2A peptide (v2Ap) of the transgene to determine timing and location of RNA expression. Using the v2Ap of the transgene is beneficial as no endogenous *ccnd1* RNA should be detected. RNA expression was seen in *ccnd1DN* embryos at 2 h pHS but was absent by 4 h pHS. The expression at 2 h pHS was located throughout most of the embryo, but was most localized in the anterior region. No expression was seen at any timepoint in the non-transgenic siblings (Figure 19).

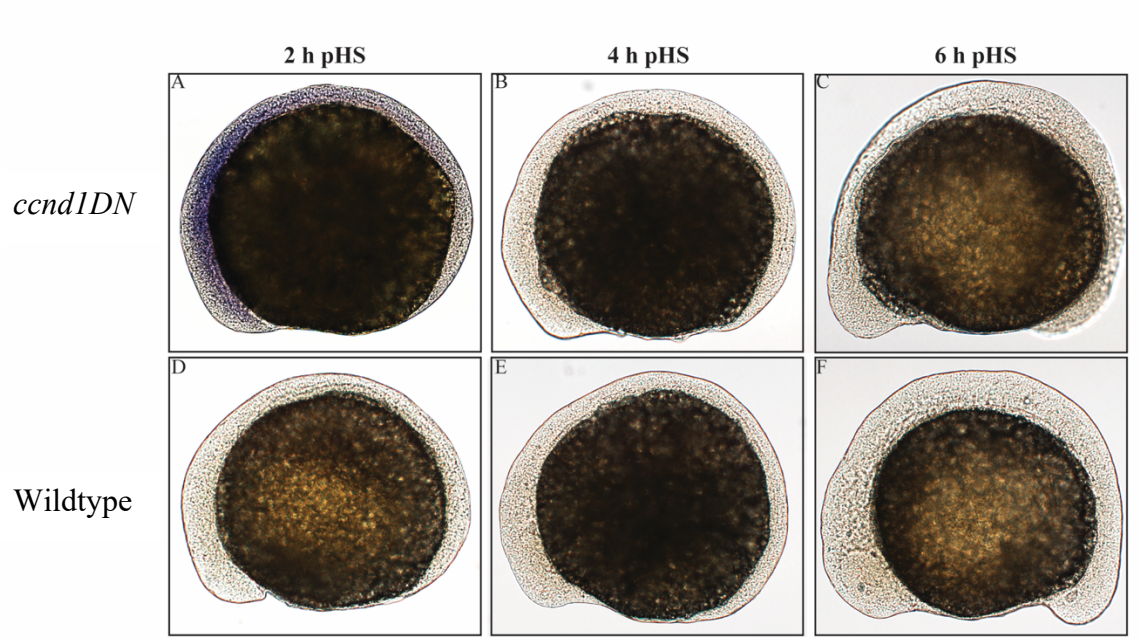

Figure 19. RNA expression of the v2Ap of the *hsp:70ccnd1DN* at 2, 4, and 6 h pHS by in situ hybridization. Expression was seen in *ccnd1DN* embryos at 2 h pHS (a) and was absent by 4 and 6 h pHS (b, c). No expression was detected in wildtype embryos (d, e, f). All embryos are oriented laterally with the head to the left.

In order to determine timing of the Ccnd1DN protein expression, western blots were attempted. Proteins were extracted from deyolked embryos 3, 6, and 9 h pHS. An anti-v2Ap antibody was used for detection as the v2Ap remains with the Ccnd1DN protein after translation and should not show expression of endogenous Ccnd1 protein. An initial attempt of a western blot performed with protein extracted at 5 h pHS, a faint band was seen at the approximate correct size of 36 kDa in the Ccnd1DN lane, with the same band absent in the lane of the non-transgenic siblings (Figure 20a). Subsequent attempts with the same western protocol and proteins extracted in the same way produced westerns with no visible proteins. This was attempted five times with no success (Figure 20b). Coomassie staining confirmed presence of protein on the gel (data not shown).

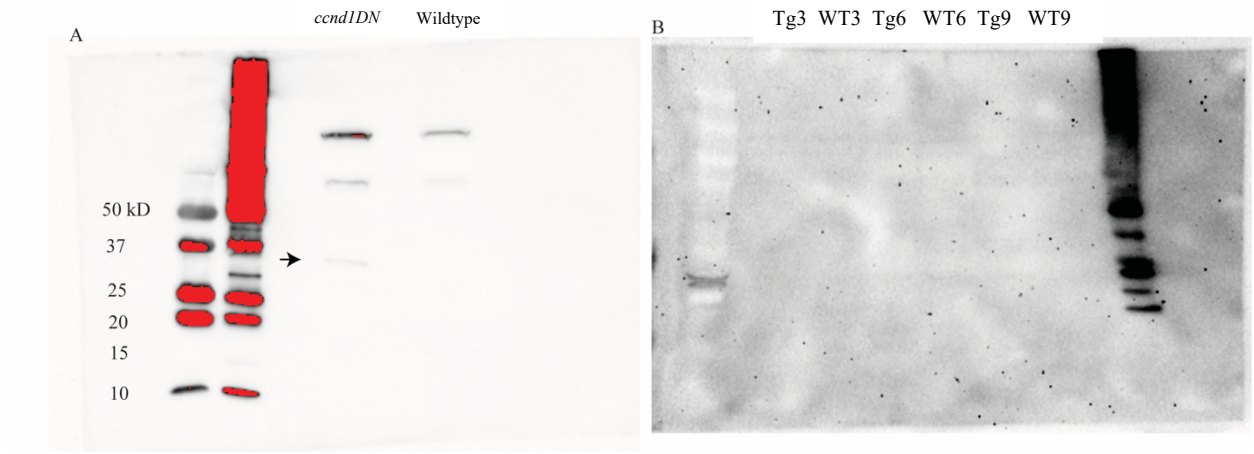

Figure 20. Western blot images attempting to detect *ccnd1DN* transgene at different time points post heat shock. Ccnd1DN and v2Ap expected to be approximately 35.58 kDa. (A) Lanes 1 and 2 show stained and unstained size markers. Lanes 3 and 4 show protein from *ccnd1DN* embryos and wildtype embryos collected at 5 h pHS. Possible band of interest indicated by arrow. (B) Subsequent attempts produced no visible proteins (size marker seen in first and last lane of gel).

Because of a lack of success using western blots to determine the timing of protein expression, immunofluorescence was used to determine both timing and location of the Ccnd1DN protein. Embryos were collected from a *ccnd1DN* x wildtype cross and sorted as transgenic or non-transgenic using fluorescence and then fixed at 3, 6, and 9 h pHS. The protein was localized to the nucleus and was detected at 3, 6, and 9 h pHS in *ccnd1DN* embryos (Figure 21). While autofluorescence can be seen in the non-transgenic siblings, no protein was detected at any timepoint in these samples. The lightest fluorescence can be seen at 3 h pHS with brighter fluorescence at 6 and 9 h pHS.

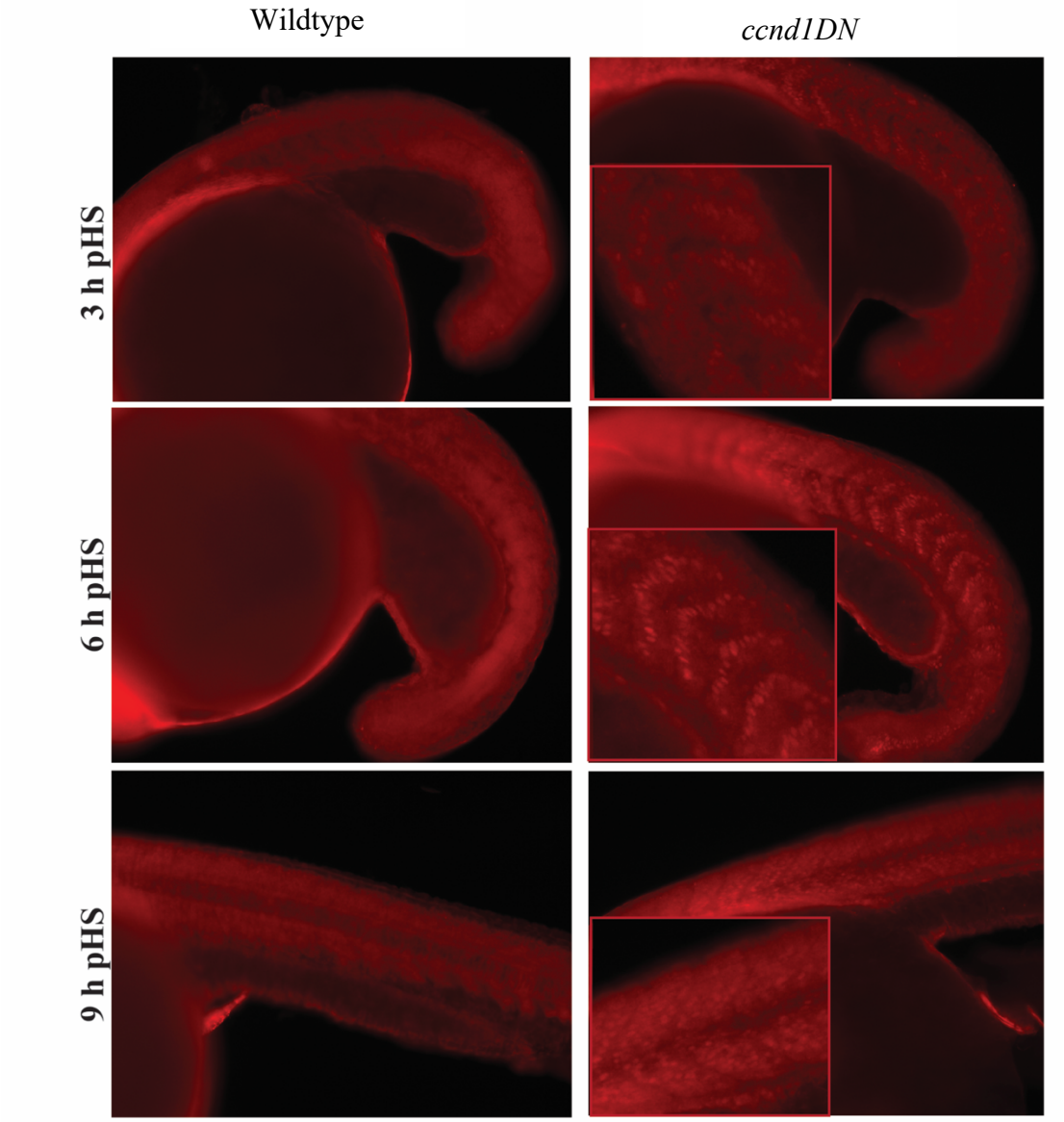

Figure 21. Expression of Ccnd1DN can be detected at 3, 6, and 9 h pHS using immunofluorescence. Inset images are magnified section of original image. All embryos oriented laterally with head to the left.

While detection of fluorescent cells was most clear along the somites of transgenic embryos, expression of Ccnd1DN can also be seen in the head. The fluorescence observed in head appears to contain more fluorescent cells than the fluorescence seen throughout the

body making the detection of individual cells more difficult. Cells can be seen in the head of 3 h pHS embryos (Figure 22) with less resolution than seen along the posterior body.

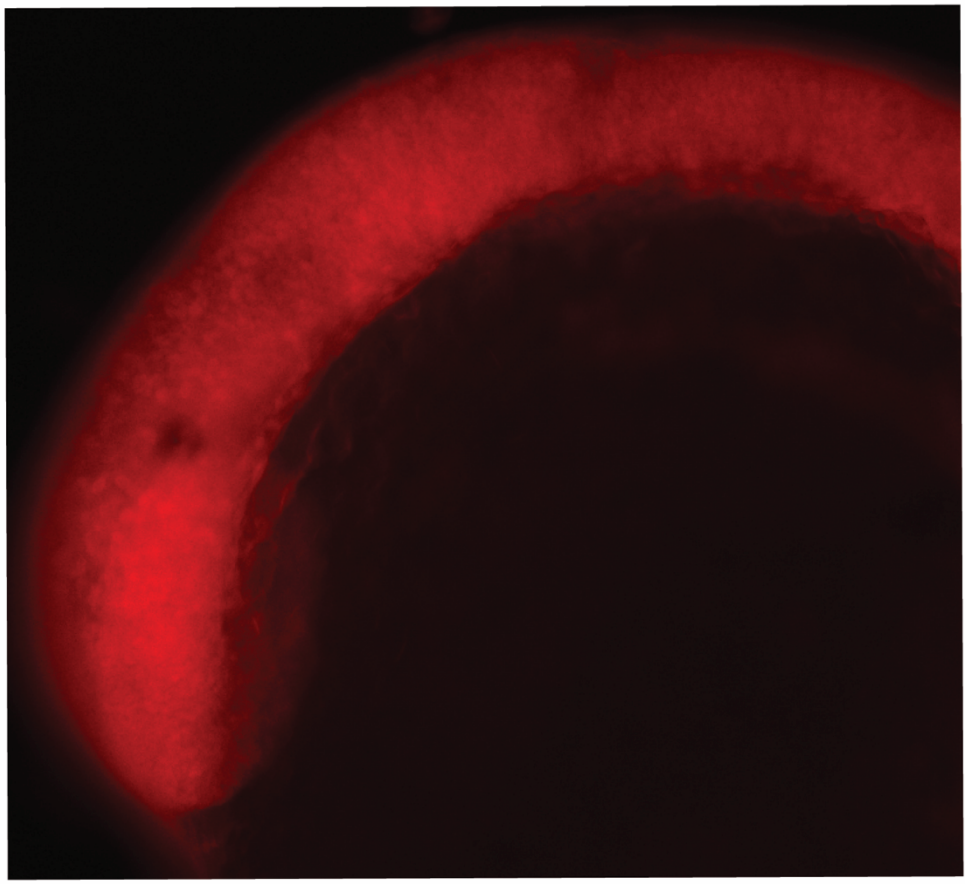

Figure 22. Expression of Ccnd1DN is seen in the head at 3 h pHS with immunofluorescence. Embryo oriented laterally with head to the left.

Genotyping the *tg(hsp70l:ccnd1DN)* and *tg(hsp70l:cdc25)* transgenic lines

The *tg(hsp70l:ccnd1DN)* line and *tg(hsp70l:cdc25)* lines each contain a Venus fluorescent reporter that is identical. Identical fluorescent reporters made it impossible to distinguish the lines from each other by fluorescence alone. This means that a reliable method of genotyping is important to separate the lines, as well as to confirm that a fish is transgenic before using it to breed to raise a new generation.

Three *ccnd1DN* and three *cdc25* fish were fin clipped and genotyped to confirm identity. Genotyping primers were designed to amplify a region of approximately 300 bp specific to the gene of interest. Wildtype DNA was used as a negative control to confirm that amplification was specific to transgenic organisms. As seen in Figure 23, when PCR is performed with *cdc25* primers, DNA isolated from *cdc25* fish produced a band at approximately 300 bp with little to no visible bands produced by *ccdn1DN* fish. When PCR is performed with *ccnd1DN* primers, DNA isolated from *ccnd1DN* fish produced a band at approximately 300 bp with little to no visible bands produced by *cdc25* fish. No 300 bp bands were seen in the AB* lane with either primer set.

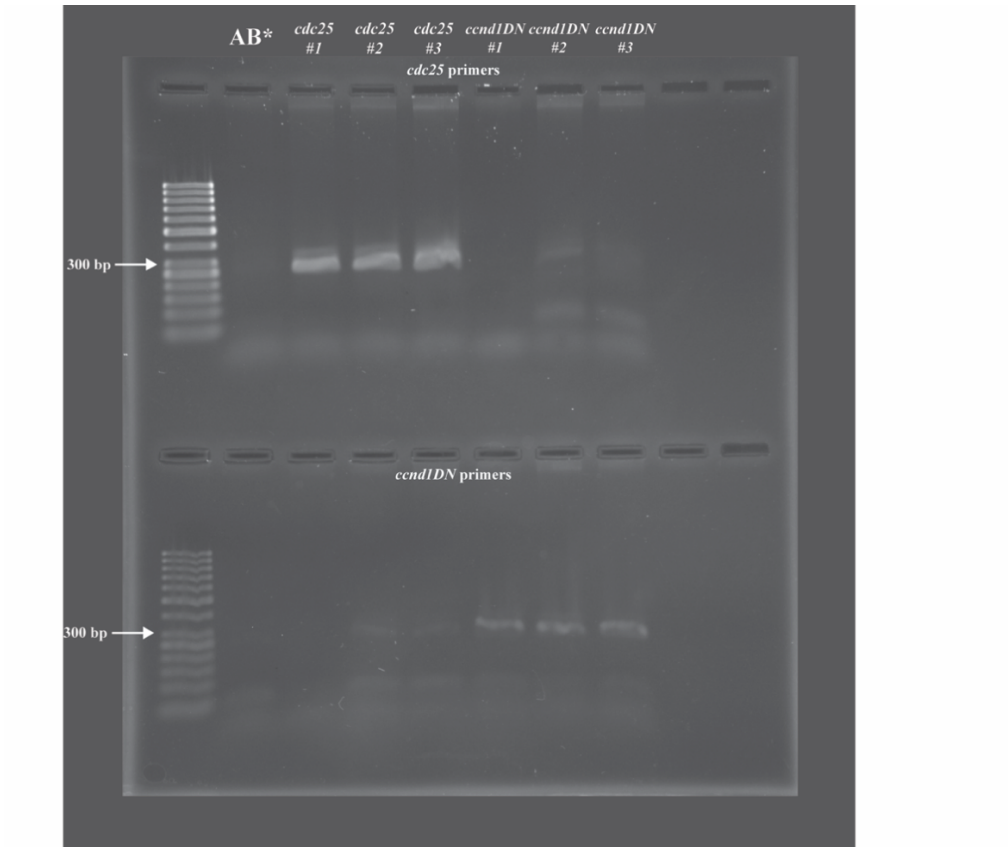

Figure 23. Genotyping PCR for *tg(hsp70l:ccnd1DN)* and *tg(hsp70l:cdc25)* transgenic lines. The first lane is a 50 bp size marker. The next lane shows the PCR product of AB* wildtype DNA with *cdc25* primers (top) or *ccnd1DN* primers (bottom). Lanes labeled *cdc25* #1-3 show the PCR product of DNA extracted from three *cdc25* fish and *cdc25* primers (top, bands seen at approximately 300 bp), or *ccnd1DN* primers (bottom, faint or no bands seen). Lanes labeled *ccnd1DN* #1-3 show the PCR product of DNA extracted from three *ccnd1DN* fish and *cdc25* primers (top, faint or no bands seen), or *ccnd1DN* primers (bottom, bands seen at approximately 300 bp).

Determining the phenotype of *tg(hsp70l:ccnd1DN)* and *tg(hsp70l:cdc25)* cross

After confirming the working order of our genotyping primers, I set out to determine the phenotype of a *tg(hsp70l:ccnd1DN)* x *tg(hsp70l:cdc25)* cross, as both lines have characterized phenotypes that offer insight into how manipulation of one of the gap phases of

the cell cycle affects development. In order to determine which transgene(s) are present after the double transgenic cross, genotyping can be used using the primers tested in Figure 23.

Previous work with the *tg(hsp70l:cdc25)* reports shortened embryos with a curved body and an average loss of seven somites (Bouldin et al., 2014). Even more straightforward for the purposes of the current study, cell death throughout the head and body is seen without injection of a p53 MO (Bouldin et al., 2014). As zebrafish have a limited breeding span of 1-2 years, new generations of *tg(hsp70l:cdc25)* fish have been raised to adulthood for continued studies. Knowing that cell death was likely to occur with the current generation, embryos from a *tg(hsp70l:cdc25)* x *tg(hsp70l:ccnd1DN)* were heat shocked at 12 somites, screened as transgenic or non-transgenic based on fluorescence, and observed for 72 hours to look for cell death. Even though cell death was initially identified by a black color in the head, after 72 hours, *cdc25* embryos remained healthy and indistinguishable from control embryos. No difference could be seen between embryos believed to have the *tg(hsp70l:cdc25)* transgene (based on fluorescence) and those without. Individual embryos were genotyped to confirm the presence of the *tg(hsp70l:cdc25)* transgene which was confirmed in approximately 50% of embryos (data not shown). Seven adult *tg(hsp70l:cdc25)* fish were genotyped and once confirmed positive, isolated DNA was sent off for sequencing. The sequencing results confirmed that the transgene was present and matched the sequence expected (data not shown).

Because the results differed from that of previous work with this line, embryos were then collected from an in-cross with the *tg(hsp70l:cdc25)* line to compare hemizygous to homozygous embryos. These embryos were heat shocked at 12 somites and sorted according

to fluorescence as transgenic or not. Cell death initially was observed in the head, but by 72 hours all embryos had recovered and cell death was no longer apparent.

The timing of the heat shock was introduced at early time points in development in an attempt to increase the severity of the effect, as the expected cell death was not observed. Embryos from a *tg(hsp70l:cdc25)* in-cross were heat shocked at 10 somites still with no effect. In a final attempt, embryos were heat shocked at 6 somites and once again screened to separate transgenics from non-transgenic siblings. At approximately 30 hpf, when embryos were 18 h pHS, embryos were imaged and no cell death was detected. Embryos were imaged again 36 h pHS, at approximately 48 hpf, when cell death should be obvious throughout the head and body, but no cell death was seen (Figure 24). Embryos were raised until 72 hpf and no developmental defects were seen (data not shown) with a 100% survival rate.

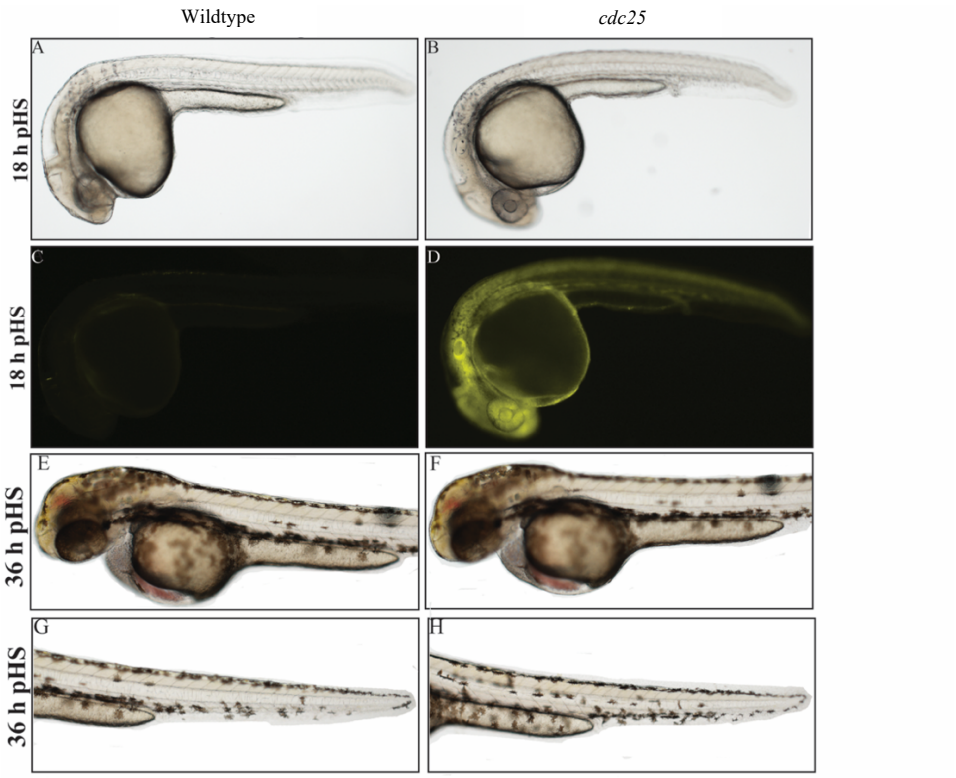

Figure 24. Embryos from a *tg(hsp70l:cdc25)* in-cross cross develop normally. Embryos were heat shocked at 6 somites and sorted according to fluorescence. No cell death was detected in embryos at 18 h pHS or 36 h pHS. All embryos are oriented with the head to the left in a lateral view. Images are representative of approximately 225 transgenic embryos and approximately 75 non-transgenic organisms.

tg(hsp70l:cdc25) cloning: Venus to tagRFP

As the current generation of *tg(hsp70l:cdc25)* fish were not showing the expected effect of the transgene believed to be caused by silencing of the gene over multiple generations, a new stable *tg(hsp70l:cdc25)* line would have to be generated again with co-injections of the *tg(hsp70l:cdc25)* construct and *tol2 transposase* mRNA. The original *tg(hsp70l:cdc25)* construct contained the fluorescent protein Venus which made it impossible to distinguish from *tg(hsp70l:ccnd1DN)* with fluorescence only, and required genotyping. To provide a faster and easier screening methods for double transgenic crosses in the future, we

decided to alter the original construct to contain a tagRFP (red fluorescent protein) instead of the Venus (a yellow fluorescent protein) previously present.

The cloning strategy for this new construct required moving tagRFP from a PCRII vector into the Tol2-containing *tg(hsp70l:cdc25)* plasmid. The Venus sequence is flanked by *SalI* and *XhoI* cut sites with an *XhoI* site also found in the PCRII vector. Primers were designed to amplify the tagRFP sequence while adding a *SalI* cut site to ensure the plasmids had compatibility which can be seen in Figure 25.

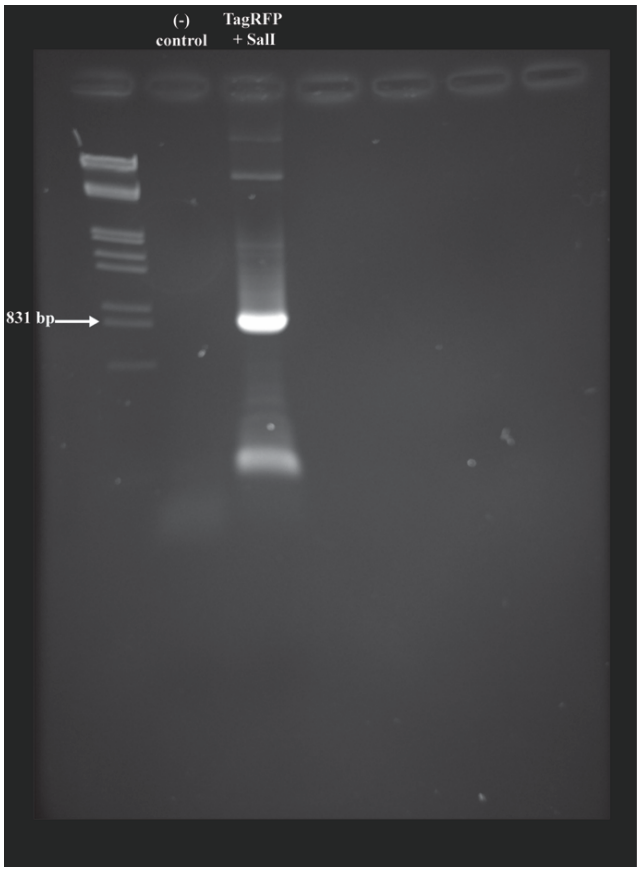

Figure 25. Gel confirmation of successful amplification of TagRFP. Lane 1 contains a λ DNA + *EcoRI* and *HindIII* size marker. Lane 2 contains a water negative control which shows no amplification. Lane 3 contains the amplified DNA seen at approximately 820 bp. The low molecular weight bands seen at the bottom of the gel are representative of primer dimers and a larger molecular weight band at the top shows original plasmid.

DISCUSSION

In order to understand the process of vertebrate development, we must understand how a single cell forms every cell type found in an adult organism. There is much research to show a relationship between the cell cycle, specifically the gap phases, and a stem cell's decision to either remain undifferentiated or differentiate into a specific cell type, like muscle cells or neurons. The Bouldin lab is interested in studying this process using neuromesodermal progenitor cells (NMPs) found in the zebrafish tailbud. NMPs have the ability to differentiate into mesoderm or ectoderm to form the posterior body of the zebrafish, including forming the somites, notochord, and spinal cord of the developing embryo. We also have the tools to investigate how NMPs are affected by manipulating the gap phases of the cell cycle using transgenic lines that manipulate the length of time cells spend in G1 (*tg(hsp70l:ccnd1DN)*) or G2 (*tg(hsp70l:cdc25)*). In the present study, I have characterized the kinetics of the *tg(hsp70l:ccnd1DN)* line in order to help determine the specific timing and location of expression to provide important information when planning experiments, as well as understand the lines affects based on known critical windows of development for specific tissues. In addition, I have investigated the expression patterns the *ntrk* family of genes required in the survival of somatosensory neurons at two timepoints, and determined how expression of *ntrk2a* changes with a prolonged G1 using the *tg(hsp70l:ccnd1DN)* line.

ntrk expression in embryonic zebrafish

While many studies exist looking at *ntrk* genes, much of the information is contradictory from one study to another. Multiple studies have suggested that each of the *ntrk*

genes are functionally distinct in zebrafish due to differential expression patterns (Martin et al., 1995; Nittoli et al., 2018), while other studies have suggested that *ntrk1, ntr2a, and ntrk3a* are all functionally similar due to overlapping expression with important nociceptive ion channels (Gau et al., 2017). Contradictory evidence shows the importance of continuing to study the early expression of the *ntrk* genes, in order to better understand their role in early development of the nervous system. The current study looked at *ntrk* expression in zebrafish at early time points in development, including 16.5 hpf, which is earlier than seen in most studies. In addition, the current study uses full-length hydrolyzed probes to provide a more accurate method of determining expression versus partial sequence probes.

Determining phylogeny was an important first step in studying the *ntrk* genes. Due to a whole-genome duplication, zebrafish have more *ntrk* genes than other vertebrates. While functionality has been determined in mice using knockout experiments (Reichardt and Fariñas, 1998), the question of functionality is much less well understood in zebrafish. Phylogeny can help determine functionality, as it would be expected that more closely related receptors share a similar function. When phylogeny has been considered previously for the *ntrk* genes, the DNA sequence is often used, even though these are protein coding genes. To get a more accurate look at how closely related the receptors are, I compared the five Trk sequences in zebrafish (*D. rerio*) to five other species (*M. musculus*, *G. gallus*, *X. tropicalis*, *H. sapiens*, and *R. norvegicus*). The *D. melanogaster* off-track gene was used to root the tree, as this is a receptor tyrosine kinase in a non-vertebrate species. The phylogenetic tree showed that *ntrk2a* and *ntrk3a* are most closely related to *Ntrk2* and *Ntrk3* in other species. While phylogenetics cannot confirm that these genes are functionally similar, it gives a better idea of which paralog may share a function with other vertebrates.

ntrk1 is unique in zebrafish in that it is the only *ntrk* gene that does not have a paralog. The teleost lineage has undergone a whole-genome duplication event (Taylor et al., 2001), and the single *ntrk1* gene found in zebrafish may be due to gene loss after the duplication (Heinrich and Lum, 2000). *Ntrk1* in mice has been shown as important for the survival of nociceptors (Reichardt and Fariñas, 1998). The present study identified *ntrk1* expression in zebrafish as early as 16.5. hpf. 16.5. hpf is an interesting time point to determine expression because this is when early embryonic patterning is in progress and one of the earliest times for specification of neurons (Kimmel et al., 1995; Metcalfe and Westerfield, 1990). Expression was determined at 16.5 hpf in two sets of cranial ganglia, with one larger set more anterior and a smaller set more posterior. Cranial ganglia expression at 16.5. hpf suggests that *ntrk1* expression is critical for the earliest specification of neurons. Expression at 24 hpf was seen in two sets of cranial ganglia as well as in the Rohon-Beard neurons along the spinal cord. While the expression of *ntrk1* has been characterized at 24 hpf, expression at 16.5 hpf has not, making the current study valuable for understanding expression when sensory neurons are first identified in the zebrafish body.

Zebrafish have two paralogs of *NTRK2, ntrk2a* and *ntrk2b*. *Ntrk2* in mice has been shown as critical for mechanoreceptor survival, with *ntrk2a* being most closely related to *Ntrk2* in other species. *ntrk2a* expression was seen in zebrafish in RB neurons and the trigeminal ganglia at both 16.5 hpf and 24 hpf. Expression of *ntrk2a* at 16.5 hpf is unique as it is the only *ntrk* gene that I saw expressed in the spinal cord at this time point and suggests an important role of *ntrk2a* in early nervous system development. Expression of *ntrk2a* in the trigeminal overlaps with expression of NGF, the TrkA ligand (Table IV; Nittoli et al., 2018). *ntrk2b* expression was detected in a completely different location from *ntrk2a*, once again

suggesting the possibility of functional differences. No expression of *ntrk2b* was detected at 16.5 hpf and expression at 24 hpf was seen in the telencephalon. Interestingly, although *ntrk2a* is most closely related to *Ntrk2*, the TrkB ligand BDNF is expressed in the telencephalon (Table VI). Ligands and receptors are expressed in different cells so overlapping expression does not necessarily mean overlapping function, but is an interesting consideration when trying to determine functionality of *ntrk2a* and *ntrk2b*, which are still unknown.

ntrk3a is the gene most closely related to *Ntrk3* in other species. In mice, *Ntrk3* has been shown to be involved in the survival of proprioceptors, but the functionality of *ntrk3a* and *ntrk3b* in zebrafish is unknown. No staining was detected in embryos at 16.5 hpf. At 24 hpf, diffuse staining can be seen in *ntrk3a* embryos throughout the head, with the most specific staining appearing to be located in the telencephalon. BDNF expression overlaps with *ntrk3a* expression in the telencephalon. Expression of *ntrk3a* can also be seen in the spinal cord. Compared to *ntrk1* and *ntrk2a*, *ntrk3a* expression appears more diffuse throughout the spinal cord instead of distinct puncta. Expression of *ntrk3b* was found in the telencephalon, midbrain, hindbrain, lateral line primordium, and otic vesicles. This expression in the telencephalon overlaps with known expression of the TrkC ligand NTF-3, as well as with NGF and NTF-3 in the otic vesicle and lateral line primordium (Table VI; Nittoli et al, 2018).

p75 NTF is a member of the tumor necrosis factor receptor superfamily and is mainly expressed early in development (Dechant and Barde, 2002). p75 can interact with all of the *ntrk* genes and can bind with low affinity to NGF, BDNF, and NTF-3, the Trk ligands. p75 complicates the idea that each Trk receptors have a modular model of function, with one of

the ligands binding to a Trk receptor to promote a specific subset of neurons. This is because p75 can promote survival of neurons as well as neuron death (Meeker and Williams, 2015). While p75 complicates the previously understood model, understanding when and where it is expressed will help with our understanding of the *ntrk* genes, including their functionality during early development. Zebrafish have two p75 homologs, *ngfra* and *ngfrb*. I elected to study expression of *ngfrb* as the sequence information was known, while *ngfra* was predicted but not known. No expression of *ngfrb* was detected at the 15 somite time point, while expression at 24 hpf can be seen in two domains of staining in the cranial ganglia. Interestingly, expression of *ngfrb* overlaps with the expression pattern determined for *ntrk1* (Table VI). TrkA has been shown to cause a prosurvival effect for p75 (Hempstead, 2002). An overlapping expression pattern between *ngfrb* and *ntrk1* would make sense as expression of both TrkA and p75 receptors in a similar location would promote neuron survival.

Table VI. *ntrk* expression overlaps with known expression patterns of the Trk ligands.

	Location of *ntrk expression*	Overlapping expression patterns	Trk receptor associated with ligand in mammals
ntrk1	two sets of cranial ganglia	p75	
ntrk2b	telencephalon	BDNF	TrkB
ntrk3a	telencephalon	BDNF	TrkB
ntrk3b	otic vesicle, telencephalon, lateral line primordium	NGF, BDNF, NTF-3	TrkA, TrkB, TrkC

Examining differences in *ntrk2a* expression in *tg(hsp70l:ccnd1DN)* embryos

Previous studies have shown a relationship between neuron specification during neurogenesis and the length of G1 (Calegari and Huttner, 2003; Canzoniere et al., 2004; Lange et al., 2009). One such study showed that cortical regions with a higher proportion of neurogenic divisions contained cells with a longer G1 phase (Lukaszewicz et al., 2005), with a short G1 being associated with a more stem-like state and a longer G1 is associated with a differentiated state. The *tg(hsp70l:ccnd1DN)* transgenic line can be used to prolong the time spent in G1 and the *ntrk* genes, which can act as markers of terminally differentiated somatosensory neurons, can be used to look for any changes in gene expression. As the *tg(hsp70l:ccnd1DN)* line prolongs the time cells spend in G1, I expected to see an increase in the number of differentiated neurons.

While it is not known how expression of any of the *ntrk* genes changes with a prolonged G1 phase, I elected to study *ntrk2a* expression, as this gene was the only *ntrk* gene I found to be expressed in the spinal cord at 16.5. hpf, and the *ntrk2a* probe gave the most robust visualization to make quantification easier and more accurate. In order to quantify the staining observed, I counted puncta along the spinal cord that were located within 1 mm from the midbrain-hindbrain boundary. Overall, I saw no significant difference in the number of puncta from wildtype to *ccnd1DN* embryos, and both samples had a high level of variance. While counting cells did not show the difference expected, other differences were noted. First was staining in the cranial ganglia. While 50% of the wildtype embryos showed two clear sets of cranial ganglia staining, this was seen in none of the *ccnd1DN* embryos. This was contradictory to the expected result, as a prolonged G1 in *ccnd1DN* was believed to produce more differentiated neurons, not fewer. In addition, studies in chick and mouse

embryos suggest that NMPs help form the neural tissue as far anteriorly as the hindbrain (Henrique et al., 2015), but the change in expression I saw extended more anteriorly than this, suggesting this change seen in cranial ganglia staining may not be a result of an altered cell cycle of NMP cells.

One question that persists with the *tg(hsp70l:ccnd1DN)* line is how the rest of the cell cycle is affected by the prolonged G1. A study in the neurons of the optic lobe in *Drosophila* suggests that it may be the overall rate of the cell cycle and not just lengthening G1 that causes the switch from proliferation to differentiation (Zhou and Luo, 2013). While *hsp70:ccdn1DN* causes an increase in the time that cells spend in G1, we do not know how other phases, like G2, are affected. If G2 is shortened to accommodate the longer G1, the overall rate of the cell cycle would remain the same, and thus explain the lack of a significant difference seen in the number of neurons. If the overall length of the cell cycle was increased due to the prolonged G1, neurons could be differentiating prematurely which could provide an explanation for the puncta of the *ccnd1DN* embryos appearing smaller than in the wildtype embryos as they could be underdeveloped.

Another possible explanation for the difference seen in cranial ganglia expression is based on changing levels endogenous levels of *ccnd1* after a heat shock. Current studies from the Bouldin lab suggest that a heat shock causes a decrease in endogenous levels of some cell cycle regulators, like *ccnd1* or *cdc25*, based on in situ hybridization data. Endogenous zebrafish *ccnd1* expression at 24 hpf is most concentrated in the head (Thisse et al., 2001). Ccnd1 levels play an important role in a cell's decision between self-renewal and differentiation, with low levels associated with a state of pluripotency, and higher levels associated with differentiation (Coronado et al., 2013). If a heat shock is causing a decrease

in endogenous *ccnd1*, where expression is most concentrated in the head, this change in expression could be affecting cells' ability to differentiate, however, this would have been seen in both the transgenic and wildtype samples. Because the transgenic embryos seem to have a decrease in neuron specification not seen in wildtype, it is possible that the wildtype are able to recover, but the prolonged gap 1 phase causes transgenic organisms to be unable to differentiate like normal. The mechanism behind this will continue to be explored. Understanding the changes in endogenous Ccnd1 and when levels return to normal will be important going forward in addition to investigating the results with a longer time course than was seen in this study.

Characterizing the kinetics of the *tg(hsp70l:ccnd1DN)* transgenic line

In order to determine timing and location of expression of the *tg(hsp70l:ccnd1DN)* transgene, I performed in situ hybridization and immunofluorescence at different time points post heat shock. For this experiment, I generated an RNA probe that is complementary to the viral 2A peptide (v2Ap) region of the transgene. Using the v2Ap sequence provides many advantages in this experiment. First, by making an RNA probe that is complementary to the v2Ap, this probe can be used with any transgenic line that contains the v2Ap sequence. For our lab, this means the probe would work with both the *tg(hsp70l:ccnd1DN)* and the *tg(hsp70l:cdc25)* lines. In addition, the v2Ap sequence would not be found in the zebrafish genome, so the results are specific to the transgene.

Using this probe, I successfully determined when and where the RNA of the *tg(hsp70l:ccnd1DN)* transgene is expressed. Embryos were heat shocked at bud stage and

RNA expression was seen 2 h pHS throughout the embryo, with the most concentrated expression seen towards the head. Expression of Ccnd1DN at 2 h pHS is consistent with the earliest detection of fluorescence. While the Ccnd1DN and Venus proteins are translated independently of each other via a ribosome skip mechanism, transcription would happen simultaneously. This means that 2 h pHS is likely when the amount of RNA present is peaking, as no expression was detected by 4 h pHS.

A reliable method for determining protein expression is important for determining the kinetics of a transgene. Similar to the 2A RNA probe, an anti-2A antibody allows for detection of the transgene without interfering with proteins naturally present and will work for any transgene with the 2A peptide sequence present. Because of the way a 2A peptide is translated, the 2A peptide will also be with the Ccnd1DN protein, making it a useful tool for determining expression of our transgene. While an anti-Venus antibody would allow for detection without the possibility of interfering with endogenous proteins, Venus and Ccnd1DN are co-translated into independent peptides and so determining expression of Venus does not provide an accurate depiction of the half-life of the Ccnd1DN protein. A common method for determining protein expression involves using western blots with extracted protein to determine the timing the protein is present, and then using immunofluorescence on whole-mount embryos for determining location.

In the current study, western blots did not give useful data on timing of the protein expression. This is likely due to too little protein in the samples. Because over 80% of proteins at this stage are yolk proteins, I attempted to deyolk embryos first to help eliminate extraembryonic proteins. While one study suggests that this improves results of western blots (Link et al., 2006), I was unable to determine timing using western blots.

Immunofluorescence has the ability to give information on both timing and location and can used in place of western blots. Using an anti-v2Ap antibody I was able to determine that the Ccnd1DN protein is expressed as early as 3 h pHS and is expressed until at least 9 h pHS with immunofluorescence. The protein was seen most clearly along the somites, where individual cells could be visualized. Fluorescence was also detected in the head, but the strong signal made it difficult to visualize individual cells. This is likely due to a higher density, as the RNA expression determined with in situ hybridization shows expression most localized in the head. In addition to overall location of the protein in the embryo, immunofluorescence allows for determination of cellular location. A previous study looking at a *Ccnd1DN* line in mice reported that the T286A mutation caused the Ccnd1DN protein to remain in the nucleus throughout the cell cycle (Alt et al., 2000). This is due to the GSK-3beta-dependent phosphorylation that normally promotes the nuclear export of Cyclin D1. As this phosphorylation is inhibited with the *ccnd1DN* line, the protein is unable to be exported from the nucleus (Alt et al., 2000). This is consistent with the immunofluorescence data in the present study that shows nuclear localization at all time points.

While previous work has confirmed that the *tg(hsp70l:ccnd1DN)* line produces the desired effect (Hung, 2015), understanding the timing and location of RNA and protein is an important next step for several reasons. First, because the transgene is under the control of a heat shock promoter, understanding the timing of transcription and translation are important for planning the timing of a heat shock. If the protein has an especially short half-life, this would have to be taken into consideration for planning experiments, as expected results may not be seen in the time frame anticipated. If the protein was degraded in an hour, the resulting effects would be seen in the development of two somites, as a new somite is formed every 30

minutes (Kimmel et al., 1995), whereas a protein with a longer half-life would produce an effect throughout development. In addition to planning experiments, understanding the kinetics of the transgene is important for interpreting results.

The process of embryogenesis involves known critical windows of development. Rohon-Beard neurons, for example, are transient cells that allow early embryos to detect information about their environment (Roberts, 2000). Most Rohon-Beard neuron precursors are found during gastrulation, and terminally differentiate by the 2 somite stage. The remaining Rohon-Beard neurons are specified post gastrulation (Rossi et al., 2009), and may come from NMPs which can contribute to formation of the spinal cord during somitogenesis (Kondoh and Takemoto, 2012). Understanding the kinetics of the transgene would be essential for determining if we would expect Rohon-Beard neurons to be affected. Another example can be seen in mesoderm with Kupffer's vesicle. This vesicle is a transient structure that appears around 5-9 somites. Fate mapping studies have determined cells of Kupffer's vesicle form notochord and muscle later on (Melby et al., 1996), so expressing Ccnd1DN during this time may produce a widespread impact on mesodermal structures.

When the present study determined *ntrk2a* expression in *tg(hsp70l:ccnd1DN)* embryos, a heat shock was performed at 16.5 hpf and left to develop until 24 hpf, 7.5 hours later. As the protein was confirmed to be expressed from 3 until at least 9 h pHS, a window of expression could be determined. During this window of expression, Rohon-Beard neurons should have been present in high numbers (Rossi et al., 2009), but it is likely that most RB neurons had already been specified at the time of transgene expression. The remaining RB neurons that are specified during segmentation could have been affected by the prolonged G1 phase caused by expression of the transgene, but in the future, looking for changes in RB

neuron expression will require a much earlier heat shock to ensure that the transgene is expressed prior to the time of specification.

Genotyping the *tg(hsp70l:ccnd1DN)* and *tg(hsp70l:ccnd1DN)* transgenic lines

Our lab has access to two previously generated transgenic lines that manipulate the length of time cells spend in one of the gap phases. Our ability to confirm the presence of the transgene is an important part in sustaining these lines, as genotyping provides an accurate method for screening fish. Because both of these lines contain a Venus fluorescent reporter, a reliable genotyping method allows for distinguishing between the lines, which fluorescence cannot do. While future experiments will hopefully generate a *tg(hsp70l:cdc25)* line that contains a TagRFP fluorescent reporter to distinguish between the lines, at the present time genotyping is required. The primers that I designed (Table II) were able to distinguish between the lines. While some non-specific banding could be seen, possibly from endogenous sequences, a clear distinction could be made, especially if positive controls were used. Further, if double transgenic organisms are generated in the future, these genotyping primers will provide a tool for determining if offspring contain one or both of the transgenes.

Determining the phenotype of *tg(hsp70l:ccnd1DN)* and *tg(hsp70l:cdc25) cross*

The *tg(hsp70l:ccnd1DN)* and *tg(hsp70l:cdc25)* lines each provide insight into how manipulation of the gap phases alters development. The *tg(hsp70l:ccnd1DN)* line produces a dominant negative form of Ccnd1 which can bind to Cdk4, but remains inactive due to a mutation that prevents phosphorylation (Diehl and Sherr, 1997). Because of this, the

tg(hsp70l:ccnd1DN) line causes a prolonged G1 phase, but only with cells in G1 or progressing from G1 into synthesis. The phenotype associated with this line consists of a smaller trunk length with fewer muscle cell nuclei, but it is difficult to determine if that is due specifically to the change in the length of G1, or if it is simply an effect of the cell dividing less often. The *tg(hsp70l:cdc25)* line expresses Cdc25 which drives cells out of G2 and into mitosis. This line produces a severe phenotype, as Cdc25 is not normally expressed in NMPs during early development, and has a phenotype of a shortened, curved body with an average loss of seven somites (Bouldin et al., 2014). While it is clear that this line has an effect on development, it is unclear whether or not cells could be compensating for the shorter G2 phase by altering the length of G1.

These questions could be addressed by a double transgenic cross which should produce one of three phenotypes. The first possibility would be a phenotype that is more severe than either individually. This result would indicate that both the short G1 and the long G2 are important for normal development, as cells would be forced out of the long G2 by Cdc25 and held in a prolonged G1 by Ccnd1DN. Another possibility would be a phenotype that looks like the *tg(hsp70l:cdc25)* phenotype indicating that the absence of a long G2 has the biggest impact and that cells can recover from the prolonged G1. The last possibility is a less severe phenotype, possibly matching the *tg(hsp70l:ccnd1DN)* phenotype indicating that cells only need to be held in a gap phase, and which gap phase is not important.

The current study was unable to determine a phenotype of a *tg(hsp70l:ccnd1DN)* x *tg(hsp70l:cdc25)* double transgenic cross due to an issue with the *tg(hsp70l:cdc25)* line. As both lines had been generated and used previously, I was able to set up a cross and collect embryos without issue. When expressed, the *tg(hsp70l:cdc25)* line has been shown to cause

cell death in the head that is followed by widespread cell death throughout the embryo without the injection of a p53 morpholino oligonucleotide. The expected results of a double transgenic cross with a heat shock during mid-somitogenesis without a p53 morpholino injection would be widespread cell death for any embryo expressing the *tg(hsp70l:cdc25)* transgene by approximately 48 hpf. When attempted initially, 100% of embryos survived up to 72 hpf and no phenotypic difference could be seen. While these embryos could be sorted as transgenic or non-transgenic based on fluorescence, it could not be determined if one or both of the transgenes were present without genotyping. Upon genotyping individual embryos, 50% of embryos were found to contain the *tg(hsp70l:cdc25)* transgene, with 1/3 being positive for both.

Because the expected results were not seen, in-crosses were set up to interbreed *tg(hsp70l:cdc25)* fish, then heat shocks were performed earlier to try to induce a more severe effect. Once again, embryos were confirmed to be transgenic using fluorescence, but all embryos survived. A heat shock was performed as early as 6 somites, but the expected results of widespread cell death were still not seen. This could to be due to gene silencing which can happen with Tol2 transgenesis. Highly repetitive sequences have been shown to be silenced after multiple generations (Goll et al., 2009). As the Tol2 sites are highly repetitive, and the transgene is inserted an average of 6 or 7 times (Urasaki et al., 2006), gene silencing could be culprit. While I was unable to complete this goal in my study, the foundation has been set for future students of the Bouldin lab.

tg(hsp70l:cdc25) cloning: Venus to tagRFP

The *tg(hsp70l:cdc25)* gene silencing provides a unique opportunity going forward with this project. As stated previously, both the *tg(hsp70l:cdc25)* and *tg(hsp70l:ccnd1DN)* lines contain the fluorescent reporter Venus for screening. While this system works well for screening individual lines, it does not allow for distinction of the two lines from each other, like in the case of a double transgenic cross. Because the *tg(hsp70l:cdc25)* line would have to be remade anyway, we saw it as a valuable opportunity to make these lines distinguishable from each other by replacing Venus with a TagRFP reporter. The cloning strategy for this consisted of moving TagRFP from a PCRII vector into the Tol2 vector with the *cdc25* gene. The Tol2 vector contained *SalI* and *XhoI* cut sites on either side of Venus. The PCRII vector contained an *XhoI* cut site, and so a plan was put into place to add a *SalI* cut site using PCR amplification. Primers were designed to amplify the entire TagRFP sequence with the addition of a *SalI* cut site, and this worked as expected. When digested Tol2 vector and TagRFP sequences were attempted to be ligated together, it was realized that these sticky ends were compatible, and the Tol2 vector was re-ligating immediately. To circumvent this, the *XhoI* cut site in the Tol2 vector was to be mutated to a *PstI* cut site, as there was already a *PstI* cut site present in the TagRFP amplified sequence and this would allow for digestion without complementary sticky ends. Mutating the sequence could be done with QuikChange site-directed mutagenesis which required designing primers 40 bp long that would have the mutation in the center. The entire sequence would be amplified, and a *DpnI* digest would remove the original methylated plasmid. While the first few rounds of QuikChange were unsuccessful, this was believed to be a result of the large size of the Tol2 vector. The *cdc25/v2Ap/venus* sequence was moved from the Tol2 vector to a smaller vector, pBluescript

KS. By designing primers to use in both the amplification TagRFP and the QuikChange PCR, as well as a plasmid with the Venus sequence in pBluescript KS, I have provided many of the materials needed for the lab to successfully complete this project.

Summary of findings

The present study sought to investigate the effect of a prolonged gap 1 phase on the specification of neuromesodermal progenitors during zebrafish embryogenesis. In order to understand the relationship between the cell cycle and stem cell differentiation, I first examined expression of a family of genes that specify sensory neurons during early development. Expression of the *ntrk* genes was found in the RB neurons, trigeminal ganglia, cranial ganglia, otic vesicle, telencephalon, midbrain, and hindbrain, with *ntrk1* and *ntrk2a* expressed as early as 16.5 hpf and *ntrk1*, *ntrk2a*, *ntrk2b*, *ntrk3a*, *ntrk3b*, and *p75* expressed at 24 hpf. Using a transgenic line of zebrafish that prolongs the gap 1 phase, I determined how *ntrk2a* expression changed from wildtype to *ccnd1DN* embryos to determine if expression changed when the cell cycle was manipulated. It was determined that the number of domains of cranial ganglia expression differs with a prolonged gap 1 phase, with smaller and fewer domains seen in transgenic organisms, as well as decreasing the size of individual puncta and causing an overall diffuse staining throughout the embryo.

In order to better understand how the *tg(hsp70l:ccnd1DN)* transgenic line works, and what structures may be affected during development, the kinetics of the *tg(hsp70l:ccnd1DN)* line were determined by looking at timing and location of RNA and protein. Using RNA in situ hybridization it was determined that RNA is expressed by 2 h pHS, and is absent by 4 h

pHS. The RNA was found to be expressed broadly, but most anteriorly. Using immunofluorescence it was determined that the Ccnd1DN protein was present at 3, 6, and 9 h pHS and localized to the nucleus. Protein stability and long half-life should allow for determining the effects of Ccnd1DN over the time scale of a cell division.

There is still work to be done in determining the phenotype of an *tg(hsp70l:cdc25)* x *tg(hsp70l:ccnd1DN)* line. Before that can be done, a future direction of the project will be to clone TagRFP into the Tol2-containing *cdc25* vector and generate a new stable transgenic line, as the gene appears to have been silenced in the previous generation. While the foundations of the project have been started, the double transgenic cross cannot happen until a new line is generated, hopefully by a Bouldin lab member in the near future. The double transgenic cross will provide our lab with important information on how the gap phase specifically affects development depending on the phenotype.

REFERENCES

Akai, J., Halley, P. A. and Storey, K. G. (2005). FGF-dependent Notch signaling maintains the spinal cord stem zone. *Genes Dev.* **19**, 2877–2887.

Alt, J. R., Cleveland, J. L., Hannink, M. and Diehl, J. A. (2000). Phosphorylation-dependent regulation of cyclin D1 nuclear export and cyclin D1-dependent cellular transformation. *Genes Dev.* **14**, 3102–3114.

Altman, J. and Das, G. D. (1965). Autoradiographic and histological evidence of postnatal hippocampal neurogenesis in rats. *J. Comp. Neurol.* **124**, 319–335.

Aoyama, H. and Asamoto, K. (1988). Determination of somite cells: independence of cell differentiation and morphogenesis. *Development* **104**, 15–28.

Bedell, V. M., Westcot, S. E. and Ekker, S. C. (2011). Lessons from morpholino-based screening in zebrafish. *Brief Funct Genomics* **10**, 181–188.

Beederman, M., Lamplot, J. D., Nan, G., Wang, J., Liu, X., Yin, L., Li, R., Shui, W., Zhang, H., Kim, S. H., et al. (2013). BMP signaling in mesenchymal stem cell differentiation and bone formation. *J Biomed Sci Eng* **6**, 32–52.

Bénazéraf, B., Chen, Q., Peco, E., Lobjois, V., Médevielle, F., Ducommun, B. and Pituello, F. (2006). Identification of an unexpected link between the Shh pathway and a G2/M regulator, the phosphatase CDC25B. *Dev. Biol.* **294**, 133–147.

Bertrand, N., Médevielle, F. and Pituello, F. (2000). FGF signalling controls the timing of Pax6 activation in the neural tube. *Development* **127**, 4837–4843.

Bianconi, E., Piovesan, A., Facchin, F., Beraudi, A., Casadei, R., Frabetti, F., Vitale, L., Pelleri, M. C., Tassani, S., Piva, F., et al. (2013). An estimation of the number of cells in the human body. *Ann. Hum. Biol.* **40**, 463–471.

Bootorabi, F., Manouchehri, H., Changizi, R., Barker, H., Palazzo, E., Saltari, A., Parikka, M., Pincelli, C. and Aspatwar, A. (2017). Zebrafish as a model organism for the development of drugs for skin cancer. *Int J Mol Sci* **18**,.

Bouldin, C. M., Snelson, C. D., Farr, G. H. and Kimelman, D. (2014). Restricted expression of cdc25a in the tailbud is essential for formation of the zebrafish posterior body. *Genes Dev.* **28**, 384–395.

Budirahardja, Y. and Gönczy, P. (2009). Coupling the cell cycle to development. *Development* **136**, 2861–2872.

Calegari, F. and Huttner, W. B. (2003). An inhibition of cyclin-dependent kinases that lengthens, but does not arrest, neuroepithelial cell cycle induces premature neurogenesis. *J. Cell. Sci.* **116**, 4947–4955.

Canzoniere, D., Farioli-Vecchioli, S., Conti, F., Ciotti, M. T., Tata, A. M., Augusti-Tocco, G., Mattei, E., Lakshmana, M. K., Krizhanovsky, V., Reeves, S. A., et al. (2004). Dual control of neurogenesis by PC3 through cell cycle inhibition and induction of Math1. *J. Neurosci.* **24**, 3355–3369.r

Cooper, G. M. (2000). *The Cell: A Molecular Approach.* Sunderland, MA: Sinauer Asociates.

Coronado, D., Godet, M., Bourillot, P.-Y., Tapponnier, Y., Bernat, A., Petit, M., Afanassieff, M., Markossian, S., Malashicheva, A., Iacone, R., et al. (2013). A short G1 phase is an intrinsic determinant of naïve embryonic stem cell pluripotency. *Stem Cell Res* **10**, 118–131.

Dechant, G. and Barde, Y.-A. (2002). The neurotrophin receptor p75(NTR): novel functions and implications for diseases of the nervous system. *Nat. Neurosci.* **5**, 1131–1136.

Del Bene, F., Wehman, A. M., Link, B. A. and Baier, H. (2008). Regulation of neurogenesis by interkinetic nuclear migration through an apical-basal Notch gradient. *Cell* **134**, 1055–1065.

Diehl, J. A. and Sherr, C. J. (1997). A dominant-negative cyclin D1 mutant prevents nuclear import of cyclin-dependent kinase 4 (CDK4) and its phosphorylation by CDK-activating kinase. *Mol. Cell. Biol.* **17**, 7362–7374.

Diez del Corral, R., Breitkreuz, D. N. and Storey, K. G. (2002). Onset of neuronal differentiation is regulated by paraxial mesoderm and requires attenuation of FGF signalling. *Development* **129**, 1681–1691.

Dréau, G. L., Saade, M., Gutiérrez-Vallejo, I. and Martí, E. (2014). The strength of SMAD1/5 activity determines the mode of stem cell division in the developing spinal cord. *J Cell Biol* **204**, 591–605.

Duesbery, N. S. V. and Woude, G. F. V. (1998). Cytoplasmic control of nuclear behavior during meiotic maturation of frog oocytes*. *Biology of the Cell* **90**, 461–466.

Edgar, B. A. and Datar, S. A. (1996). Zygotic degradation of two maternal Cdc25 mRNAs terminates Drosophila's early cell cycle program. *Genes Dev.* **10**, 1966–1977.

Escudero, L. M. and Freeman, M. (2007). Mechanism of G1 arrest in the Drosophila eye imaginal disc. *BMC Dev Biol* **7**, 13.

Evans, M. J. and Kaufman, M. H. (1981). Establishment in culture of pluripotential cells from mouse embryos. *Nature* **292**, 154–156.

Fantl, V., Stamp, G., Andrews, A., Rosewell, I. and Dickson, C. (1995). Mice lacking cyclin D1 are small and show defects in eye and mammary gland development. *Genes Dev.* **9**, 2364–2372.

Farioli-Vecchioli, S., Mattera, A., Micheli, L., Ceccarelli, M., Leonardi, L., Saraulli, D., Costanzi, M., Cestari, V., Rouault, J.-P. and Tirone, F. (2014). Running rescues defective adult neurogenesis by shortening the length of the cell cycle of neural stem and progenitor cells. *Stem Cells* **32**, 1968–1982.

Forsburg, S. L. and Nurse, P. (1991). Cell cycle regulation in the yeasts Saccharomyces cerevisiae and Schizosaccharomyces pombe. *Annu. Rev. Cell Biol.* **7**, 227–256.

Foudi, A., Hochedlinger, K., Van Buren, D., Schindler, J. W., Jaenisch, R., Carey, V. and Hock, H. (2009). Analysis of histone 2B-GFP retention reveals slowly cycling hematopoietic stem cells. *Nature Biotechnology* **27**, 84–90.

Gau, P., Curtright, A., Condon, L., Raible, D. W. and Dhaka, A. (2017). An ancient neurotrophin receptor code; a single Runx/Cbfβ complex determines somatosensory neuron fate specification in zebrafish. *PLoS Genet.* **13**, e1006884.

Georgopoulou, N., Hurel, C., Politis, P. K., Gaitanou, M., Matsas, R. and Thomaidou, D. (2006). BM88 is a dual function molecule inducing cell cycle exit and neuronal differentiation of neuroblastoma cells via cyclin D1 down-regulation and retinoblastoma protein hypophosphorylation. *J. Biol. Chem.* **281**, 33606–33620.

Gilbert, S. F. (2000). *Developmental Biology*. Sunderland, MA: Sinauer Associates.

Glasauer, S. M. K. and Neuhauss, S. C. F. (2014). Whole-genome duplication in teleost fishes and its evolutionary consequences. *Mol. Genet. Genomics* **289**, 1045–1060.

Goll, M. G., Anderson, R., Stainier, D. Y. R., Spradling, A. C. and Halpern, M. E. (2009). Transcriptional Silencing and Reactivation in Transgenic Zebrafish. *Genetics* **182**, 747–755.

Goto, H., Kimmey, S. C., Row, R. H., Matus, D. Q. and Martin, B. L. (2017). FGF and canonical Wnt signaling cooperate to induce paraxial mesoderm from tailbud neuromesodermal progenitors through regulation of a two-step epithelial to mesenchymal transition. *Development* **144**, 1412–1424.

Gould, K. L. and Nurse, P. (1989). Tyrosine phosphorylation of the fission yeast cdc2+ protein kinase regulates entry into mitosis. *Nature* **342**, 39–45.

Graña, X. and Reddy, E. P. (1995). Cell cycle control in mammalian cells: role of cyclins, cyclin dependent kinases (CDKs), growth suppressor genes and cyclin-dependent kinase inhibitors (CKIs). *Oncogene* **11**, 211–219.

Griffiths, A. J., Miller, J. H., Suzuki, D. T., Lewontin, R. C. and Gelbart, W. M. (2000). *An Introduction to Genetic Analysis.* New York: W. H. Freeman.

Hao, S., Chen, C. and Cheng, T. (2016). Cell cycle regulation of hematopoietic stem or progenitor cells. *Int. J. Hematol.* **103**, 487–497.

Hara, K., Tydeman, P. and Kirschner, M. (1980). A cytoplasmic clock with the same period as the division cycle in Xenopus eggs. *Proc Natl Acad Sci U S A* **77**, 462–466.

Hardwick, L. J. A., Ali, F. R., Azzarelli, R. and Philpott, A. (2015). Cell cycle regulation of proliferation versus differentiation in the central nervous system. *Cell Tissue Res* **359**, 187–200.

Hartwell, L. H. (1967). Macromolecule synthesis in temperature-sensitive mutants of yeast. *J. Bacteriol.* **93**, 1662–1670.

Hartwell, L. H., Culotti, J. and Reid, B. (1970). Genetic Control of the Cell-Division Cycle in Yeast, I. Detection of Mutants. *Proc Natl Acad Sci U S A* **66**, 352–359.

Heinrich, G. and Lum, T. (2000). Fish neurotrophins and Trk receptors. *International Journal of Developmental Neuroscience* **18**, 1–27.

Hempstead, B. L. (2002). The many faces of p75NTR. *Curr. Opin. Neurobiol.* **12**, 260–267.

Henrique, D., Abranches, E., Verrier, L. and Storey, K. G. (2015). Neuromesodermal progenitors and the making of the spinal cord. *Development* **142**, 2864–2875.

Holtzhausen, A., Golzio, C., How, T., Lee, Y.-H., Schiemann, W. P., Katsanis, N. and Blobe, G. C. (2014). Novel bone morphogenetic protein signaling through Smad2 and Smad3 to regulate cancer progression and development. *FASEB J* **28**, 1248–1267.

Homem, C. C. F. and Knoblich, J. A. (2012). Drosophila neuroblasts: a model for stem cell biology. *Development* **139**, 4297–4310.

Horowitz, N. H. and Leupold, U. (1951). Some recent studies bearing on the one geneone enzyme hypothesis. *Cold Spring Harb. Symp. Quant. Biol.* **16**, 65–74.

Huang, E. J. and Reichardt, L. F. (2001). Neurotrophins: roles in neuronal development and function. *Annu. Rev. Neurosci.* **24**, 677–736.

Hung, K. L. (2015). A Prolonged G1 Phase of The Cell Cycle Affects Muscle and Blood Vessel Formation during Zebrafish Development. *Honors thesis,* University of Washington, Seattle, WA.

Jagannathan-Bogdan, M. and Zon, L. I. (2013). Hematopoiesis. *Development* **140**, 2463–2467.

Jirmanova, L., Afanassieff, M., Gobert-Gosse, S., Markossian, S. and Savatier, P. (2002). Differential contributions of ERK and PI3-kinase to the regulation of cyclin D1 expression and to the control of the G1/S transition in mouse embryonic stem cells. *Oncogene* **21**, 5515–5528.

Kimmel, C. B., Ballard, W. W., Kimmel, S. R., Ullmann, B. and Schilling, T. F. (1995). Stages of embryonic development of the zebrafish. *Dev. Dyn.* **203**, 253–310.

Kishimoto, M., Fukui, T., Suzuki, R., Takahashi, Y., Sumimoto, K., Okazaki, T., Sakao, M., Sakaguchi, Y., Yoshida, K., Uchida, K., et al. (2015). Phosphorylation of Smad2/3 at specific linker threonine indicates slow-cycling intestinal stem-like cells before reentry to cell cycle. *Dig. Dis. Sci.* **60**, 362–374.

Kishimoto, T. (2015). Entry into mitosis: a solution to the decades-long enigma of MPF. *Chromosoma* **124**, 417–428.

Kondoh, H. and Takemoto, T. (2012). Axial stem cells deriving both posterior neural and mesodermal tissues during gastrulation. *Curr. Opin. Genet. Dev.* **22**, 374–380.

Kozar, K., Ciemerych, M. A., Rebel, V. I., Shigematsu, H., Zagozdzon, A., Sicinska, E., Geng, Y., Yu, Q., Bhattacharya, S., Bronson, R. T., et al. (2004). Mouse development and cell proliferation in the absence of D-cyclins. *Cell* **118**, 477–491.

Lange, C., Huttner, W. B. and Calegari, F. (2009). Cdk4/cyclinD1 overexpression in neural stem cells shortens G1, delays neurogenesis, and promotes the generation and expansion of basal progenitors. *Cell Stem Cell* **5**, 320–331.

Lee, H. O. and Norden, C. (2013). Mechanisms controlling arrangements and movements of nuclei in pseudostratified epithelia. *Trends Cell Biol.* **23**, 141–150.

Lee, M. G. and Nurse, P. (1987). Complementation used to clone a human homologue of the fission yeast cell cycle control gene cdc2. *Nature* **327**, 31–35.

Link, V., Shevchenko, A. and Heisenberg, C.-P. (2006). Proteomics of early zebrafish embryos. *BMC Dev Biol* **6**, 1.

Liu, X., Huang, J., Chen, T., Wang, Y., Xin, S., Li, J., Pei, G. and Kang, J. (2008). Yamanaka factors critically regulate the developmental signaling network in mouse embryonic stem cells. *Cell Res.* **18**, 1177–1189.

Lobjois, V., Benazeraf, B., Bertrand, N., Medevielle, F. and Pituello, F. (2004). Specific regulation of cyclins D1 and D2 by FGF and Shh signaling coordinates cell cycle progression, patterning, and differentiation during early steps of spinal cord development. *Dev. Biol.* **273**, 195–209.

Lodish, H., Berk, A., Zipursky, S. L., Matsudaira, P., Baltimore, D. and Darnell, J. (2000). Biochemical studies with oocytes, eggs, and early embryos. *Molecular Cell Biology.* New York: W. H. Freeman.

Lohka, M. J., Hayes, M. K. and Maller, J. L. (1988). Purification of maturation-promoting factor, an intracellular regulator of early mitotic events. *Proceedings of the National Academy of Sciences of the United States of America* **85**, 3009.

Lukaszewicz, A., Savatier, P., Cortay, V., Giroud, P., Huissoud, C., Berland, M., Kennedy, H. and Dehay, C. (2005). G1 phase regulation, area-specific cell cycle control, and cytoarchitectonics in the primate cortex. *Neuron* **47**, 353–364.

Magnusson, J. P. and Frisén, J. (2016). Stars from the darkest night: unlocking the neurogenic potential of astrocytes in different brain regions. *Development* **143**, 1075–1086.

Malumbres, M., Sotillo, R., Santamaría, D., Galán, J., Cerezo, A., Ortega, S., Dubus, P. and Barbacid, M. (2004). Mammalian cells cycle without the D-type cyclin-dependent kinases Cdk4 and Cdk6. *Cell* **118**, 493–504.

Martin, B. L. and Kimelman, D. (2012). Canonical Wnt signaling dynamically controls multiple stem cell fate decisions during vertebrate body formation. *Dev. Cell* **22**, 223–232.

Martin, G. R. (1981). Isolation of a pluripotent cell line from early mouse embryos cultured in medium conditioned by teratocarcinoma stem cells. *Proc. Natl. Acad. Sci. U.S.A.* **78**, 7634–7638.

Martin, S. C., Marazzi, G., Sandell, J. H. and Heinrich, G. (1995). Five Trk receptors in the zebrafish. *Developmental Biology* **169**, 745–758.

Martin, S. C., Sandell, J. H. and Heinrich, G. (1998). Zebrafish TrkC1 and TrkC2 receptors define two different cell populations in the nervous system during the period of axonogenesis. *Dev. Biol.* **195**, 114–130.

Masui, Y. and Markert, C. L. (1971). Cytoplasmic control of nuclear behavior during meiotic maturation of frog oocytes. *J. Exp. Zool.* **177**, 129–145.

Meeker, R. B. and Williams, K. S. (2015). The p75 neurotrophin receptor: at the crossroad of neural repair and death. *Neural Regen Res* **10**, 721–725.

Megason, S. G. and McMahon, A. P. (2002). A mitogen gradient of dorsal midline Wnts organizes growth in the CNS. *Development* **129**, 2087–2098.

Melby, A. E., Warga, R. M. and Kimmel, C. B. (1996). Specification of cell fates at the dorsal margin of the zebrafish gastrula. *Development* **122**, 2225–2237.

Metcalfe, W.K. and Westerfield, M. (1990). *Systems Approaches to Developmental Neurobiology.* New York: Plenum Press.

Mitchison, J. M. (1990). The fission yeast, Schizosaccharomyces pombe. *Bioessays* **12**, 189–191.

Molina, A. and Pituello, F. (2017). Playing with the cell cycle to build the spinal cord. *Dev. Biol.* **432**, 14–23.

Morgan, D. O. (1995). Principles of CDK regulation. *Nature* **374**, 131–134.

Morgan, D.O. (2007). *The Cell Cycle: Principles of control.* London: New Science Press Ltd.

Murray, A. W. and Kirschner, M. W. (1989). Cyclin synthesis drives the early embryonic cell cycle. *Nature* **339**, 275.

Nittoli, V., Sepe, R. M., Coppola, U., D'Agostino, Y., De Felice, E., Palladino, A., Vassalli, Q. A., Locascio, A., Ristoratore, F., Spagnuolo, A., et al. (2018). A comprehensive analysis of neurotrophins and neurotrophin tyrosine kinase receptors expression during development of zebrafish. *J. Comp. Neurol.* **526**, 1057–1072.

Nogare, D. E. D., Arguello, A., Sazer, S. and Lane, M. E. (2007). Zebrafish cdc25a is expressed during early development and limiting for post-blastoderm cell cycle progression. *Developmental Dynamics* **236**, 3427–3435.

Nurse, P., Thuriaux, P. and Nasmyth, K. (1976). Genetic control of the cell division cycle in the fission yeast Schizosaccharomyces pombe. *Molec. Gen. Genet.* **146**, 167–178.

Olivera-Martinez, I. and Storey, K. G. (2007). Wnt signals provide a timing mechanism for the FGF-retinoid differentiation switch during vertebrate body axis extension. *Development* **134**, 2125–2135.

Orford, K. W. and Scadden, D. T. (2008). Deconstructing stem cell self-renewal: genetic insights into cell-cycle regulation. *Nat. Rev. Genet.* **9**, 115–128.

Passegué, E., Wagers, A. J., Giuriato, S., Anderson, W. C. and Weissman, I. L. (2005). Global analysis of proliferation and cell cycle gene expression in the regulation of hematopoietic stem and progenitor cell fates. *J. Exp. Med.* **202**, 1599–1611.

Pauklin, S. and Vallier, L. (2013). The cell-cycle state of stem cells determines cell fate propensity. *Cell* **155**, 135–147.

Pauklin, S. and Vallier, L. (2015). Activin/Nodal signalling in stem cells. *Development* **142**, 607–619.

Pauklin, S., Madrigal, P., Bertero, A. and Vallier, L. (2016). Initiation of stem cell differentiation involves cell cycle-dependent regulation of developmental genes by Cyclin D. *Genes Dev.* **30**, 421–433.

Phillips, J. (2017). Cell Cycle Manipulation: Quantifying Effects of an Extended G1 Phase on Circulation in Developing *Danio Rerio*. *Honors Thesis*, Appalachian State University, Boone, NC.

Philpott, A. and Yew, P. R. (2005). The Xenopus cell cycle: an overview. *Methods Mol. Biol.* **296**, 95–112.

Purves, D., Augustine, G. J., Fitzpatrick, D., Katz, L. C., LaMantia, A.-S., McNamara, J. O. and Williams, S. M. (2001). *Neuroscience.* Sunderland, MA: Sinauer Associates.

Qiu, J., Papatsenko, D., Niu, X., Schaniel, C. and Moore, K. (2014). Article: Divisional History and Hematopoietic Stem Cell Function during Homeostasis. *Stem Cell Reports* **2**, 473–490.

Reichardt, L. F. and Fariñas, I. (1998). *Neurotrophic factors and their receptors: Roles in neuronal development and function*. Oxford, UK: Oxford University Press.

Reyes, R., Haendel, M., Grant, D., Melancon, E. and Eisen, J. S. (2004). Slow degeneration of zebrafish Rohon-Beard neurons during programmed cell death. *Dev. Dyn.* **229**, 30–41.

Roberts, A. (2000). Early functional organization of spinal neurons in developing lower vertebrates. *Brain Res. Bull.* **53**, 585–593.

Rossi, C. C., Kaji, T. and Artinger, K. B. (2009). Transcriptional control of Rohon-Beard sensory neuron development at the neural plate border. *Dev. Dyn.* **238**, 931–943.

Rubinfeld, B., Souza, B., Albert, I., Müller, O., Chamberlain, S. H., Masiarz, F. R., Munemitsu, S. and Polakis, P. (1993). Association of the APC gene product with beta-catenin. *Science* **262**, 1731–1734.

Santoriello, C. and Zon, L. I. (2012). Hooked! Modeling human disease in zebrafish. *J. Clin. Invest.* **122**, 2337–2343.

Seita, J. and Weissman, I. L. (2010). Hematopoietic stem cell: self-renewal versus differentiation. *Wiley Interdiscip Rev Syst Biol Med* **2**, 640–653.

Siegrist, S. E. and Doe, C. Q. (2006). Extrinsic cues orient the cell division axis in Drosophila embryonic neuroblasts. *Development* **133**, 529–536.

Sugiyama, M., Sakaue-Sawano, A., Iimura, T., Fukami, K., Kitaguchi, T., Kawakami, K., Okamoto, H., Higashijima, S. and Miyawaki, A. (2009). Illuminating cell-cycle progression in the developing zebrafish embryo. *Proc. Natl. Acad. Sci. U.S.A.* **106**, 20812–20817.

Szymczak, A. L., Workman, C. J., Wang, Y., Vignali, K. M., Dilioglou, S., Vanin, E. F. and Vignali, D. A. A. (2004). Correction of multi-gene deficiency in vivo using a single "self-cleaving" 2A peptide-based retroviral vector. *Nat. Biotechnol.* **22**, 589–594.

Takizawa, H., Regoes, R. R., Boddupalli, C. S., Bonhoeffer, S. and Manz, M. G. (2011). Dynamic variation in cycling of hematopoietic stem cells in steady state and inflammation. *The Journal Of Experimental Medicine* **208**, 273–284.

Taylor, J. S., Van de Peer, Y., Braasch, I. and Meyer, A. (2001). Comparative genomics provides evidence for an ancient genome duplication event in fish. *Philos Trans R Soc Lond B Biol Sci* **356**, 1661–1679.

Thisse, B., Pflumio, S., Fürthauer, M., Loppin, B., Heyer, V., Degrave, A., Woehl, R., Lux, A., Steffan, T., Charbonnier, X.Q. and Thisse, C. (2001) Expression of the zebrafish genome during embryogenesis (NIH R01 RR15402). ZFIN Direct Data Submission (http://zfin.org).

Urasaki, A., Morvan, G. and Kawakami, K. (2006). Functional dissection of the Tol2 transposable element identified the minimal cis-sequence and a highly repetitive sequence in the subterminal region essential for transposition. *Genetics* **174**, 639–649.

Vermeulen, K., Van Bockstaele, D. R. and Berneman, Z. N. (2003). The cell cycle: a review of regulation, deregulation and therapeutic targets in cancer. *Cell Prolif.* **36**, 131–149.

Westerfield, M. (2000). *The zebrafish book. A guide for the laboratory use of zebrafish (Danio rerio)*. Eugene, OR: Univ. of Oregon Press.

Wilson, A., Laurenti, E., Oser, G., van der Wath, R. C., Blanco-Bose, W., Jaworski, M., Offner, S., Dunant, C. F., Eshkind, L., Bockamp, E., et al. (2008). Hematopoietic stem cells reversibly switch from dormancy to self-renewal during homeostasis and repair. *Cell* **135**, 1118–1129.

Yasutis, K. M. and Kozminski, K. G. (2013). Cell cycle checkpoint regulators reach a zillion. *Cell Cycle* **12**, 1501–1509.

Ying, Q.-L., Wray, J., Nichols, J., Batlle-Morera, L., Doble, B., Woodgett, J., Cohen, P. and Smith, A. (2008). The ground state of embryonic stem cell self-renewal. *Nature* **453**, 519–523.

Zhang, Z., Chang, L., Yang, J., Conin, N., Kulkarni, K. and Barford, D. (2013). The four canonical tpr subunits of human APC/C form related homo-dimeric structures and stack in parallel to form a TPR suprahelix. *J. Mol. Biol.* **425**, 4236–4248.

Zhou, L. and Luo, H. (2013). Replication protein a links cell cycle progression and the onset of neurogenesis in Drosophila optic lobe development. *J. Neurosci.* **33**, 2873–2888.

Vita

Katie Michelle Hahn was born in Pueblo, Colorado to Lisa and Cayle Hahn. She graduated from Johnston County Middle County High School in Smithfield, North Carolina in 2013. The following autumn she attended Appalachian State University and received a Bachelor of Science degree in Cell and Molecular Biology in 2017. In the fall of 2017, she continued at Appalachian State University to obtain a Master of Science degree in Cell and Molecular Biology where she is scheduled to graduate in August 2019.